MODELLING POLLUTANT EMISSIONS IN DIESEL ENGINES, INFLUENCE OF BIOFUEL ON POLLUTANT FORMATION

Zvonimir Petranović*, Tibor, Bešenić, Milan Vujanović, Neven Duić

Faculty of Mechanical Engineering and Naval Architecture
University of Zagreb, Ivana Lučića 5, Zagreb, Croatia
e–mail: zvonimir.petranovic@fsb.hr, tibor.besenic@fsb.hr, milan.vujanovic@fsb.hr, neven.duic@fsb.hr

ABSTRACT

In order to reduce the harmful effect on the environment, European Union allowed using the biofuel blends as fuel for the internal combustion engines. Experimental studies have been carried on, dealing with the biodiesel influence on the emission concentrations, showing inconclusive results. In this paper numerical model for pollutant prediction in internal combustion engines is presented. It describes the processes leading towards the pollutant emissions, such as spray particles model, fuel disintegration and evaporation model, combustion and the chemical model for pollutant formation. Presented numerical model, implemented in proprietary software FIRE®, is able to capture chemical phenomena and to predict pollutant emission concentration trends. Using the presented model, numerical simulations of the diesel fuelled internal combustion engine have been performed, with the results validated against the experimental data. Additionally, biodiesel has been used as fuel and the levels of pollutant emissions have been compared to the diesel case. Results have shown that the biodiesel blends release lower nitrogen oxide emissions than the engines powered with the regular diesel.

Keywords: Diesel engine; Biodiesel, Combustion; Spray process; CFD

1. INTRODUCTION

During operation of Internal Combustion (IC) diesel engines a vast amount of fossil fuel is consumed, and therefore they represent a threat to the environment in terms of pollutant emissions. In theoretical conditions, when the complete fuel combustion is achieved, solely the CO_2 and H_2O species would be generated. However, such conditions are impossible to achieve due to the engine transient operating conditions. In 2013, 25% of the global CO_2 emissions originated from the transportation sector (Energy Agency, 2015). In addition, as a consequence of IC engine operating conditions, several other species, such as CO, HC, PM and NO_x, are produced. Relative to the total flue gases flow, 1% belong to these species, of which approximately 50% are the NO_x species (Khair and Majewski, 2006).

As a part of the tendency towards cleaner transport sector with lower impact on the environment, concentrations of the emitted pollutant emissions have been regulated in the past decade (Klemeš et al., 2012), and more stringent conditions are enforced by the governmental policies every year. Comparing to the spark ignition engines, the diesel engines are characterised by greater energy conversion and safety factor (Katrašnik, 2007). In order to remain the most used vehicle powering

* Corresponding author. Tel.: +385 1 6168 494; fax: +385 1 6156 940.
E-mail address: zvonimir.petranovic@fsb.hr (Z. Petranovic).

source on the European market, as well as to meet the higher efficiency standards, the IC engines efficiency must be constantly improved (Kozarac et al., 2014). In addition to the emission regulations, another obstacle for IC engine utilisation is the promotion of biofuels in the transportation sector (Niemisto et al., 2013). As a part of the European biofuels directive (2003/30/EC) in 2003, a minimum level of used biofuels was enforced to all EU member states. Recently, the European Standards Committee (CEN) allowed the maximum amount of bio – content up to 7%, and even a higher values are expected in the near future. Biodiesel is derived by transesterification, does not contain sulphur, degrades quickly, and is nontoxic (Tashtoush et al., 2007). In addition to the engine performance optimisation, NO emissions can be reduced by introducing various exhaust gas recirculation and engine boosting systems. A good review regarding exhaust particle filter technologies is shown in (Guan et al., 2015).

The combustion process within the IC diesel engine can be divided into two distinguished parts: the uncontrollable premixed combustion which takes place during the autoignition process, and mixing-controlled diffusion combustion. Most of the vaporised fuel is combusted in the diffusion regime and therefore the overall engine efficiency highly depends on the spray process. The spray is a highly transient and turbulent multiphase process, which consists of several distinguished processes, such as fuel jet disintegration, droplet atomization and collision, an evaporation process, air entrainment, etc.

Spray is a versatile process, apart from the internal combustion engines also used in removing pollutant emissions (Baleta et al., 2016), and the numerous experimental investigations have been performed. However, with the progress of computational power and development of Computational Fluid Dynamic (CFD) tools, combining experimental research with CFD analysis became the common approach. With such approach, an understanding of complex and transient turbulent flows that are hard to capture experimentally can be significantly improved. For the reliable use of CFD tools, each of the used submodels should be previously validated. Finally, combining the CFD tools with experimental research could result in a reduction of the overall expenses and investigation duration.

There are various approaches developed for the computational modelling of turbulent dispersed multiphase flows, such as Direct Numerical Simulation (DNS) for the particles, the Discrete Particle Model (DPM), the Euler-Lagrangian (EL), and the Euler Eulerian (EE) model, etc. (Martin Sommerfeld, Berend van Wachem, 2008). The EL approach is the most used approach for modelling the spray process. While it suffers from several disadvantages, such as mesh dependency, parallel calculation efficiency reduction, high particle loading (Petranović et al., 2015), the EL approach is sufficiently accurate and efficient for modelling the diluted spray region, as shown for the liquids by Faeth et al. (Faeth et al., 1995), as well as for solid particles (Mikulčić et al., 2016). In order to overcome its disadvantages, the EE approach can be used (Vujanović et al., 2016)(Petranović et al., 2017). Within EE approach both the liquid and the gas phases are treated as a continuum. For improved accuracy, the discrete phase is sorted into a finite number of classes, characterised by the mean droplet diameter (FIRE manual 2013, 2013). The phase interaction is achieved through source terms in the conservation equations accounting for the droplet dynamics. Despite the increased computational power requirements compared to the EL approach, the EE approach is suitable for modelling all spray regimes, including the dense spray region.

To overcome disadvantages inherent to the EL and the EE approaches, they can be coupled by using the AVL FIRE® Code Coupling Interface (ACCI) (von Berg et al., 2005)(Edelbauer, 2014)(Vujanović et al., 2016) or through the ELSA modelling concept (Vallet et al., 2001). The difference between these modelling concepts is that in the ACCI approach, the gas and the liquid phases in the vicinity of the nozzle are treated separately, and within the ELSA model they are treated as one mixture phase.

Available literature on usage of biodiesel blends as fuel in compression-ignition engines generally reports decrease in particulate matter (PM), hydrocarbon (HC) and carbon monoxide (CO) emissions as benefits, as well as increased levels of NO_x emissions as one of the main drawbacks of biodiesel implementation (Giakoumis et al., 2012). However, a deeper insight into reported experimental results questions this increasing trend and analyses its causes. For example, a comprehensive literature review (Lapuerta et al., 2008) examines differences in fuel injection and combustion due to disparities in physical and chemical properties of biodiesel, such as lower heating value, bulk modulus and viscosity etc. It is similarly (Sun et al., 2010) concluded that, although the increase in NO_x production exists, it is not inherent to the biofuel itself, but rather due to the usage of biodiesel in unmodified diesel engine setups. This way, the difference in biodiesel properties advances the start of injection process and increases the combustion temperatures, leading to the elevated NO_x emissions. In real-life experimental setups, it is often hard to ensure consistent operational parameters when comparing different fuels (e.g. the same start and the end of injection). In these situations, numerical simulations can be a great tool for analysis and comparison of performances of different fuels in the same working regimes.

It is one of this papers' aims to numerically investigate the NO_x pollutant emissions when using biodiesel blends, compared to the identical conditions with regular diesel fuel. Therefore, it is important to understand the thermochemical phenomena behind the formation of NO_x. Nitrogen-containing emissions from the combustion processes are commonly classified as thermal, prompt, and fuel NO_x, relative to the mechanism of their production (Vujanović, 2010). Thermal NO_x forms by dissociation of the molecular nitrogen from the air and is highly temperature-dependent, prompt NO_x occurs in nitrogen reactions with hydrocarbon radicals in the first stages of reactions, and the fuel NO_x is formed by complex reaction paths from nitrogen contained in the fuel. In modern CFD approaches, NO_x emissions are almost invariantly modelled as a post-processing step after calculation of the flow field and main combustion. This is justified by the, in absolute terms, small concentrations of NOx, which have a low impact on overall flow field, temperature and concentrations of major combustion products, as well as by different time scales of the fast combustion reactions and the relatively slower production of NO_x (Hill and Smoot, 2000). Although detailed kinetic mechanisms exist (Miller and Bowman, 1989), in order to obtain the computationally efficient model, some simplifications need to be made. Chemical model simplifications, such as omitting the species with negligible concentrations, removing reaction paths with minute influence on the overall NO_x production or the assumption of chemical equilibrium are a common approach to simplifying complex chemical phenomena for usage in CFD. Reduced number of chemical equations allows for an efficient coupling with the turbulent reacting flow. Chemistry-turbulence interaction was modelled by taking into the account temperature fluctuations, integrating the chemical reaction rates and applying the Probability Density Function (PDF) approach (Vujanović et al., 2009). Presented numerical model for modelling NO_x emissions has been implemented in the CFD code FIRE.

The paper is structured as follows: first, the description of the available experimental data is given. Later, the short introduction into the Euler-Lagrangian spray modelling is provided, together with the NO_x modelling equations. Afterwards, the numerical setup is described and the results are thoroughly discussed. Finally, the conclusions are drawn in section 'Conclusions'.

2. AVAILABLE EXPERIMENTAL DATA

To find the most suitable NO_x modelling approach, the single cylinder engine was computationally modelled. This engine is designed as a Single CYlinder ENgine (SCYLEN), with electro-hydraulic valve actuation, and the ω-shaped piston. The main SCYLEN engine and injector system characteristics are shown in Table 1.

Table 1 Engine specifications

Bore (mm)	85	**Spray Angle (°)**	158
Stroke (mm)	94	**Displacement (mm^3)**	533.4
Compression ratio (-)	16:1	**Nozzle (-)**	8-hole
Nozzle location (mm)	2,0,-3.8	**Inj. Pressure (bar)**	1200-1600
Orifice diameter (mm)	0.1		

For the research purposes several engine operating points were examined, and the main combustion parameters are shown in Table 2.

Table 2 Engine combustion parameters

Case	SOI – EOI (°CA)	Swirl (1/min)	Injected mass (kg)	EGR mass fraction (%)
a	712.5 – 735.4	5832	3.37×10^{-6}	23.84
b	713.5 – 734.4	5544.6	3.41×10^{-6}	19.68
c	712.5 – 735.4	5832	3.37×10^{-6}	23.84
d	712.5 – 733.4	4030.2	3.4×10^{-6}	23.5
e	713.4 – 736.1	4048.2	3.38×10^{-6}	23.36
f	714.4 – 736.9	4072.8	3.38×10^{-6}	16.16

Table 3 shows the measured NO_x and soot emission concentrations expressed per kilogramme of exhaust gases measured at the time of exhaust valve opening. The pressure measurements have been carried out using the PUMA Open system, whilst the pollutant emissions have been measured using the AVL emission measurement system.

Table 3 Measured emission concentrations

Case	Soot (kg/kg)	NO (kg/kg)	Case	Soot (kg/kg)	NO (kg/kg)
a	2.09×10^{-5}	5.62×10^{-4}	d	2.50×10^{-5}	4.33×10^{-4}
b	1.67×10^{-5}	5.55×10^{-4}	e	5.28×10^{-5}	3.43×10^{-4}
c	6.64×10^{-5}	3.64×10^{-4}	f	1.92×10^{-5}	5.60×10^{-4}

3. NUMERICAL MODEL

To calculate the spray process occurring inside the IC engine combustion chamber the EL approach was used. In such approach, the gas phase is treated as the continuous phase in the Eulerian framework, whilst the Lagrangian formulation is used to describe the discrete phase dynamics. In the Lagrangian formulation samples of individual droplets with the same physical properties and dimensions are tracked through the domain. These samples are commonly known as parcels (Dukowicz, 1980). The grouping procedure, in comparison to tracking each fuel droplet, reduces the overall computational effort. Following expression is used to calculate parcel trajectory:

$$\rho_l \frac{du_P}{dt} = \sum F , \tag{1}$$

where the terms on the left-hand side are the density and the parcel acceleration, whilst the term on the right-hand side represents the forces acting on the droplet parcel *P*. The force term may get its contribution from drag, gravity, buoyancy, pressure difference, and external forces. In the observed application, the main force that results in droplet momentum dissipation is the drag force.

3.1. Spray submodels

By injecting the liquid fuel with high velocity through small diameter nozzle holes, fuel is subject to the atomization process. The atomization is driven by the occurrence of the surface instabilities which are a consequence of the aerodynamic and turbulent forces. As a result, a population of small diameter droplets is distributed within the combustion chamber, which is later evaporated and combusted. Next sections show brief introduction into models utilised for a description of the spray process.

3.1.1. Fuel disintegration

Liquid sprays are used in various technical applications, such as internal combustion engines, gas turbines, spray painting, spray cooling, fire extinction, waste treatment, spray quenching, spray drying (Cusidó and Cremades, 2012), etc. In this research, the liquid fuel was injected through the high-pressure injection systems that generate high-velocity fluid motion, and therefore we employed the WAVE disintegration model. The used WAVE disintegration model considers the occurrence of surface instabilities due to the Kelvin-Helmholtz (KH) and Rayleigh-Taylor (RT) instabilities. The RT instabilities are a result of the acceleration of dense medium by the less dense one, whilst KH instabilities are a result of shear forces acting on the droplet surface. To match experimental data, the WAVE model offers two distinguished modelling constants, where one constant is correlating the diameter of created droplet with the wavelength of the fastest surface instability, and other is used to correct the breakup time, according to next equations:

$$r_{stable} = B_0 \Lambda \tag{2}$$

$$\tau_a = 3.726 B_1 \frac{r_k}{\Lambda_k \Omega_k} , \tag{3}$$

where r_{stable} is the target diameter, B_0 is the modelling constant, Λ is the wavelength of the surface instability, τ_a is the atomization time scale, B_1 is the modelling constant, r_k is the droplet diameter, and Ω is the surface instability growth rate. The Λ and Ω are in a function on local flow properties and they are calculated by using the semi empirical (Reitz, 1987):

$$\Lambda_k = 9.02 r_k \frac{\left(1+0.45\cdot Oh^{0.5}\right)\left(1+0.4\cdot T^{0.7}\right)}{\left(1+0.87\cdot We_1^{1.67}\right)^{0.6}} \tag{4}$$

$$\Omega_k = \left(\frac{\rho_k r_k^{\,3}}{\sigma}\right)^{-0.5} \frac{0.34+0.38\cdot We_1^{1.5}}{\left(1+Oh\right)\left(1+1.4\cdot T^{0.6}\right)}, \tag{5}$$

where Oh is is the Ohnesorge number, T is the Taylor number, and We_1 is the gas phase Weber number. The mass loss due to the atomization process is shown with next equation:

$$\frac{dm_k}{dt} = 4\pi r_k^{\,2} \rho_k \frac{dr_k}{dt}\ , \tag{6}$$

where term on the left side of the equation is the mass loss of class k, ρ_k is the fuel density and last term is the artificial diameter reduction defined as:

$$\frac{dr_k}{dt} = -\frac{r_k - r_{\text{target}}}{\tau_A},\ r_{\text{target}} \le r_k\ . \tag{7}$$

3.1.2. Fuel evaporation

In this research, the Dukowicz evaporation model was employed to predict the discrete phase heating and evaporation (Dukowicz, 1979). This model assumes that the droplet is spherical in shape and a steady quasi-film is present around the droplet surface. The droplet has infinite conductivity, uniform physical properties are assumed in the surrounding gas, and the thermal equilibrium is assumed on the droplet surface. The disadvantage of the Dukowicz evaporation formulation is that it is suitable for predicting evaporation when the ratio of thermal diffusivity to mass diffusivity is equal to unity and that it is not capable of predicting the condensation of the gas species. However, for the observed application, this model is capable of predicting the evaporation process, which will be shown in the result section.

3.1.3. Momentum exchange

As it was previously mentioned, the drag force is the main contributor to momentum exchange between the continuous and the discrete phase. The drag force is calculated according to the following expression:

$$F_D = \frac{\rho_g}{2} c_D A_D u_{rel}^{\,2}, \tag{8}$$

where ρ_g is gas phase density, term c_D is the drag coefficient, A_D is projected area, and u_{rel} the gas-liquid relative velocity. To model the drag coefficient of a single sphere, in this research the following formulation was used (Schiller and Naumann, 1933):

$$c_D = \begin{cases} \frac{24}{\mathrm{Re}}\left(1+0.15\cdot \mathrm{Re}^{0.687}\right) \rightarrow \ for\ \mathrm{Re} \le 1000 \\ 0.44 \rightarrow \ for\ \mathrm{Re} > 1000 \end{cases}. \quad (9)$$

3.1.4. Spray-wall interaction

In operation of diesel engines, the spray-wall interaction may have a significant role, especially for small bore engines where the distance between injector and piston surface is small. To take into account the droplet behaviour after a collision with the piston surface, approaches such as the wall interaction model or the wall film physics can be employed. In this research, the authors utilised the wall film module where parcel rebound/reflection is modelled depending on the Weber number (Naber and Reitz, 1988).

3.1.5. Droplet collision

From the viewpoint of the statistical particle method, which is the basis of the EL spray approach, the droplet collision process is modelled by a statistical approach. The most common approach is the O'Rourke collision model (O'Rourke, 1989), which has disadvantages such as mesh dependency. To overcome mesh dependency disadvantage, we employed the approach developed by Nordin (Nordin, 2001), which is an improvement of the O'Rourke approach (*FIRE manual 2013*, 2013).

3.2. The pollutant formation model

3.2.1. The NO_x model

Significant amounts of nitrogen-containing pollutants are emitted in the environment with the combustion of diesel fuels. Nitrogen oxides is the collective term for the family of seven polluting chemical compounds: nitrogen monoxide (NO), nitrogen dioxide (NO_2), nitrous oxide (N_2O), dinitrogen dioxide (N_2O_2), dinitrogen trioxide (N_2O_3), dinitrogen tetroxide (N_2O_4) and dinitrogen pentoxide (N_2O_5) (Vujanović, 2010). Diesel combustion releases NO_x emissions predominantly as NO, with levels of other nitrogen species in the negligible amounts (Scheffknecht et al., 2011). Therefore, all of the NO_x emissions are modelled as NO. For tracking the NO species concentrations, transport equation below was solved.

$$\frac{\partial(\bar{\rho}\tilde{Y}_{\mathrm{NO}})}{\partial t} + \frac{\partial(\tilde{u}_i\bar{\rho}\tilde{Y}_{\mathrm{NO}})}{\partial x_i} = \frac{\partial}{\partial x_i}\left(\bar{\rho}D_t\frac{\partial\tilde{Y}_{\mathrm{NO}}}{\partial x_i}\right) + \bar{S}_{\mathrm{NO}}. \quad (10)$$

On the left-hand side, the first term describes the temporal change of the NO concentrations, and the second one shows convection change. On the right-hand side, the first term describes the diffusive change, while the last term stands for the source of NO. Generally, the aforementioned nitrogen oxides formation mechanisms together comprise the NO source term, as seen in Eq. (11). Thermal mechanism forms nitrogen oxides in post-flame regions by oxidation of nitrogen, prompt

NO is formed in reactions of molecular nitrogen with hydrocarbon radicals, and the fuel NO occurs as the result of the several parallel reaction paths from the fuel contained nitrogen. However, in compression-ignition engine applications fuel NO is considered irrelevant (Mobasheri et al., 2012). Thus, the source term S_{NO} is comprised only of the most influential reaction mechanisms – the thermal and the prompt NO – and third term in Eq. (11) equals zero. Terms inside the brackets stand for the temporal concentration changes for thermal, prompt and fuel NO respectively, and M_{NO} is the NO molar mass.

$$S_{NO} = M_{NO}\left(\frac{dc_{NOthermal}}{dt} + \frac{dc_{NOprompt}}{dt} + \frac{dc_{NOfuel}}{dt}\right) \tag{11}$$

Thermal NO concentrations are highly influenced by the local temperature. The strong triple covalent bonds of the molecular nitrogen from the air have high activation energy that needs to be exceeded for the reaction to proceed. For this reason, dissociation of nitrogen is considered to be the rate-limiting step of the thermal reaction mechanism. Another parameter that thermal NO depends greatly upon is the concentration of the O and OH radicals. Reported numerical models almost invariantly use three chemical equations of the extended Zeldovich mechanism (Zeldovich et al., 1947) for modelling the thermal NO emissions. Reaction in Eq. (12) describes dissociation of the molecular nitrogen contained in the air by the oxygen radicals. Nitrogen produced this way is oxidised (Eq. 13) and further reacts with the OH radicals that can have high concentrations in fuel-rich conditions (Eq. 14).

$$N_2 + O \overset{k_1}{\leftrightarrow} NO + N \tag{12}$$

$$N + O_2 \overset{k_2}{\leftrightarrow} NO + O \tag{13}$$

$$N + OH \overset{k_3}{\leftrightarrow} NO + H \tag{14}$$

Both forward and backwards chemical reaction rate coefficients for above three equations are modelled according to the Arrhenius law. Further model simplification is the assumption of the quasi-steady-state for the nitrogen atoms. This way atomic nitrogen is consumed as fast as it is produced, and the overall thermal NO source can be simplified (*FIRE manual 2013*, 2013).
Contrary to the slower and temperature-dependent thermal NO formation, prompt NO – firstly described by the Fenimore (Fenimore, 1971) – forms earlier by the fast reactions of nitrogen in the fuel-rich regions. In the combustion process fuel is fragmented into the hydrocarbon radicals, denoted by the overall formula CH_i, that react with nitrogen and form hydrogen cyanide (HCN). HCN then participates in a series of rapid reactions and is subsequently oxidised to produce NO (Petranović et al., 2015).

$$CH_i + N_2 \longleftrightarrow HCN + N + \cdots \tag{15}$$

Overall prompt NO is described by the expression in Eq. (16), which provides improved results by including the correction factor obtained from comparison with experimental data (Vujanović, 2010).

$$\frac{dc_{\mathrm{NO}}}{dt} = k \; f c_{\mathrm{O_2}}{}^{b} c_{\mathrm{N_2}} c_{fuel} \exp\left(-\frac{E}{RT}\right) \tag{16}$$

The impact of the turbulent fluctuations of temperature and species concentrations on NO production is highly nonlinear. Their effect is taken into account by considering Probability Density Function (PDF). PDF is assumed to be a two-moment beta function, as appropriate for combustion calculations. It is defined as in Eq. (17.), with B being the beta function, and the α and β being functions of the mean temperature and its variance, obtained by solving transport equation for variance of temperature (Vujanović, 2010):

$$P(T) = \frac{T^{\alpha-1}(1-T)^{\beta-1}}{B(\alpha,\beta)} = \frac{\Gamma(\alpha+\beta)}{\Gamma(\alpha)\Gamma(\beta)} T^{\alpha-1}(1-T)^{\beta-1}. \tag{17}$$

Gamma function Γ is defined according to the following:

$$\Gamma(z) = \int_0^\infty e^{-t} t^{z-1} dT. \tag{18}$$

Finally, the mean turbulent rate of production of NO is obtained by Eq. (19), where $S_{Y_{NO}}$ is the integrated instantaneous rate of production.

$$\overline{S}_{Y_{NO}} = \int_0^1 P(T) S_{Y_{NO}}(T) dT \tag{19}$$

3.2.2. The soot model

At high temperatures and fuel-rich conditions, hydrocarbon fuels show the tendency to form carbonaceous particles, otherwise known as soot. The soot is formed in the early stage of the engine working cycle, but it is later oxidised. To model the soot formation rate, the transport equation for the soot mass fraction is solved. In this work, the Kinetic soot model characterised with a reduced number of species and reactions was employed. The basis of used soot model is a soot chemical reaction mechanism that covers approximately 1850 homogeneous reactions, 186 species and 100 heterogeneous reactions (*FIRE manual 2013*, 2013).

4. CALCULATION SETTINGS AND NUMERICAL SETUP

Spray process was modelled by using the EL spray modelling approach, whilst the combustion process was modelled by employing the common ECFM-3Z combustion model (*FIRE manual 2013*, 2013). Such model is a reasonable choice in modelling the IC Diesel engine since it correctly describes both the premixed and diffusion flames. Several engine operating points were simulated, as shown in Table 2 and Table 3. The detailed information on the nozzle flow conditions was not known and authors assumed non-cavitating symmetrical nozzle flow conditions. Therefore, the CFD simulations were performed on engine segment mesh covering 1/8 (45°) of the cylinder bowl

and one nozzle hole, as can be seen in Figure 1. With aforementioned assumption, the CPU costs were significantly reduced.

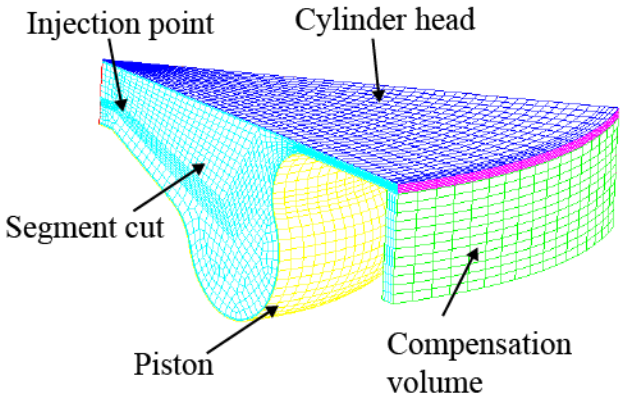

Figure 1 Generated computational mesh with defined selections

The liquid fuel was injected from the certain point of the computational domain in the direction defined by the nozzle geometry, as defined in Table 1. For all operating conditions, the cylinder head and piston selection were defined as non-permeable wall boundary conditions with a constant temperature of 500 and 550 K, respectively. To achieve the real engine compression ratio, compensation volume selection had to be generated since the computational domain was simplified, comparing to the real chamber geometry. Only one segment of the whole chamber was modelled and therefore the periodic boundary condition was applied to the segment cut selection. The generated computational mesh contains approximately 23800 control volumes in the Top Dead Centre (TDC) and 67500 control volumes in the Bottom Dead Centre (BDC). The piston selection was defined as moving mesh which resulted in deformation of certain computational cells. Therefore, the mesh was rezoned several times to satisfy predefined conditions of aspect ratio and cell orthogonality.

The Central Differencing Scheme (CDS) was used for discretization of the continuity equation, and the Upwind Differencing Scheme (UDS) was used for turbulence, energy and scalar transport equations. The blend between the CDS and UDS differencing schemes with blending factor of 0.5 was used for the momentum equations. The turbulence was modelled by using the advanced $k-\zeta-f$ turbulence model (Hanjalić et al., 2004). This model is robust enough and can be used for simulations with moving computational meshes and swirled compressed flows, as it is the case in the observed engineering application.

5. RESULTS AND DISCUSSION

The initial step of this research was to find the most suitable NO production mechanism for the observed IC engine configuration, and the results are shown in Figure 2. Around the TDC the local in-cylinder temperatures reach over 2000 K, which is high enough to break strong triple bonds of the N_2 species. Therefore, the thermal mechanism was employed on two different engine operating points and compared with the experimental data. The results of NO concentrations with only thermal NO mechanism are shown for operating points *a* and *b*, where rather big discrepancies with the experimental data are noticeable. To increase the accuracy of CFD simulations, production of NO species by the prompt mechanism was introduced. Characteristic for the prompt

mechanism is that generation of NO occurs earlier than NO produced by the thermal mechanism, and it usually increases the overall NO concentrations. For both of the mentioned NO modelling approaches, the NO emissions are calculated from the mean or averaged quantities, which can be improved by coupling the NO generation with the turbulence. Therefore, the effect of turbulence was introduced through the PDF of temperature variance which improved the prediction of absolute NO concentrations for all engine operating points.

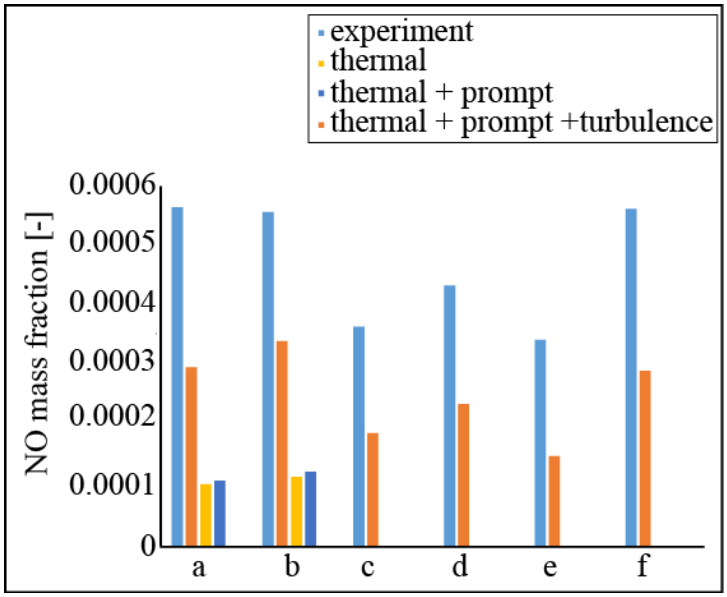

Figure 2 **NO_x concentrations for different modelling approaches compared with the experimental data**

For a correct prediction of the absolute NO emissions, a more detailed IC engine simulation should be performed. In presented modelling cases some simplifications exist that could have an impact on pollutant emission modelling. It is well known that NO prediction is influenced by:

- Nozzle flow conditions: the authors acquired the injection rate from the experimental research. This information could be improved by information such as mass flow distribution between nozzle holes, generation of vapour phase through the cavitation process, real inlet boundary conditions such as temperature, volume fractions of discrete and continuous phase, etc. It is known that nozzle flow can have a significant impact on the overall spray shape and thus, it can influence the fuel-air mixing, combustion, and pollutant formation.
- Spray shape: for more detailed results, quantities such as liquid and vapour penetrations should be acquired for spray parameterization. Also, information such as axial and radial mixture distribution, spray angle, droplet distribution, etc. would be beneficial. Aforementioned information should be acquired at least for one engine case, or for artificial constant volume case with similar parameters to tune the spray submodels. It is a known fact that in IC engine the combustion is mostly mixing-driven and therefore, spray plays a major role in predicting the temperature development, which finally dictates the NO generation and destruction rate.

- The used combustion model which is thoroughly validated on many applications could be replaced with detailed, skeletal or reduced chemistry mechanism.
- The boundary and the initial conditions that are taken from the experimental research as a mean value. This could be improved by simulating suction stroke where information such as swirl number, turbulent kinetic energy and dissipation rate, etc. would be acquired for the whole engine cycle. Also, mesh topology could include the injector and valve heads volumes, which would lead to the removal of compensation volume shown in Figure 1.

Due to simplification of the engine model, it is more reasonable to track the trend of pollutant emissions. This implies that the relative change of NO and soot concentrations with engine operating conditions modification is of greater interest. The emission trends are shown in Figure 3, where a good agreement with the experimental data is achieved, both for the NO and soot emissions.

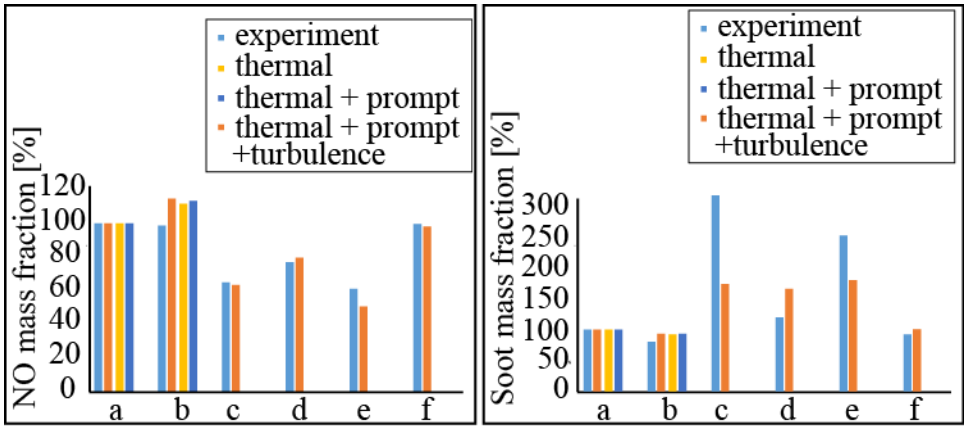

Figure 3 Normalised pollutant concentrations for different modelling approaches compared with the experimental data

In the last step of the research, diesel fuel was replaced with the EN590B7 mixture, which is a blend of diesel with 7% of fatty acid methyl esters (FAME), and performed the CFD simulations for all operating points. Here, the thermal and prompt NO mechanisms were employed, with the turbulence interactions included through the PDF function. The results of biodiesel addition for observed engine configuration are shown in Figure 4, where similar levels of NO concentrations were obtained for both fuels. The trend with changing engine operating conditions is the same for both fuels, but the biofuel addition exhibits lower values of absolute NO concentrations. The averaged decrease in predicted NO mass fraction with the addition of the biofuel is 8.02%.
These results differ from the greater part of the experimental data from the literature, where NO concentration increases are reported when using biodiesel. It should be noted, as was mentioned before, that experimental results were obtained by simply replacing the fuels and thus altering the start and the end of injection – considered the main culprit for the temperature change and the NO emission increase. In the present work, all of the simulation parameters were kept the same, which is crucial for the valid comparison of the results.

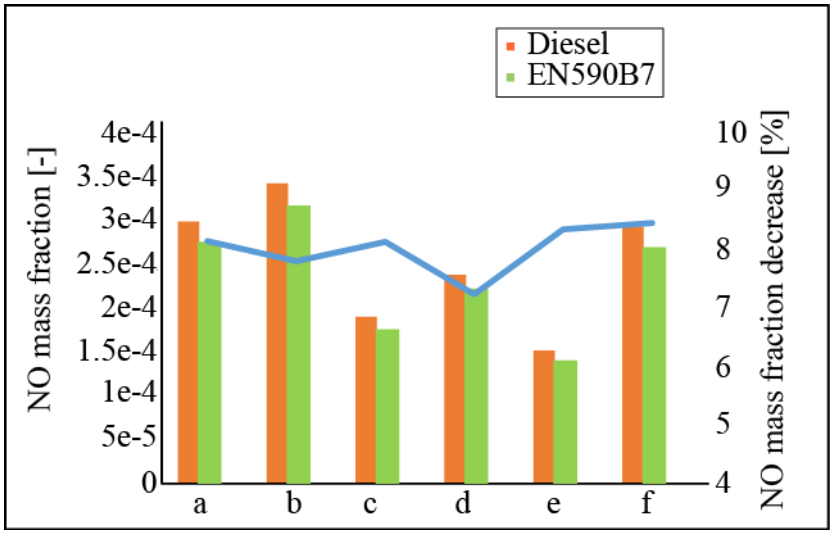

Figure 4 NO concentrations reduction due to biofuel addition

Figure 5 shows the mean pressure and temperature profiles for the engine compression and expansion strokes. It can be seen that the calculated results are in an excellent agreement with the measured data. The pressure and temperature rise due to a reduction in engine working volume in the compression stroke. At a certain crank angle position, few degrees before TDC, the liquid fuel is injected into the cylinder. The liquid fuel disintegrates into small diameter droplets and evaporates, which is visible in temperature reduction due to the heat consumed. After the fuel vapour is produced and mixed with the hot gas mixture, ignition starts and in-cylinder pressure and temperature rise rapidly. At 720° the piston moves towards BDC and the working volume is increased, leading to pressure and temperature reduction.

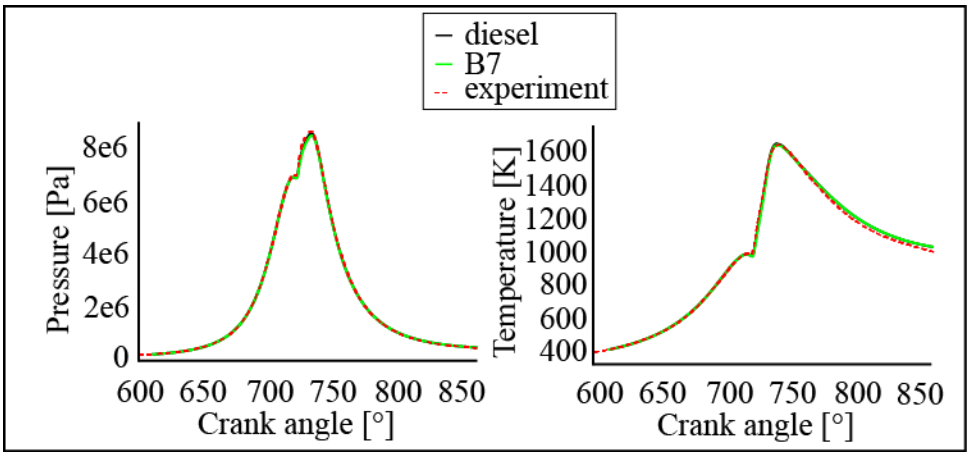

Figure 5 Mean pressure and temperature profiles

At later crank angle positions when a significant amount of vapour mass is produced and mixed with the hot surrounding gases, the exothermic chemical reactions occur. The release of heat through the chemical reactions – the combustion process, lead to a rapid temperature increase at a certain location within the combustion chamber. The combustion process starts at the periphery of the vapour cloud, as visible in Figure 6. This figure shows isosurface of vapour mass fraction coloured with the temperature of surrounding gas phase, and the isosurface representing the gas

phase temperature of at least 1600 K. The results obtained with the injection of diesel fuel and diesel biofuel blend shows similar occurrence of the combustion process around 722 °CA, and later flame consumes the vapour cloud towards the injector. The development of high-temperature contour is visible at crank positioned at 725 °CA. In the conducted simulations, the combustion process occurs slightly earlier and it is more pronounced in the case of pure diesel fuel combustion. A more progressive combustion process leads to higher local in – cylinder temperatures, and thus higher concentrations of pollutant NO species.

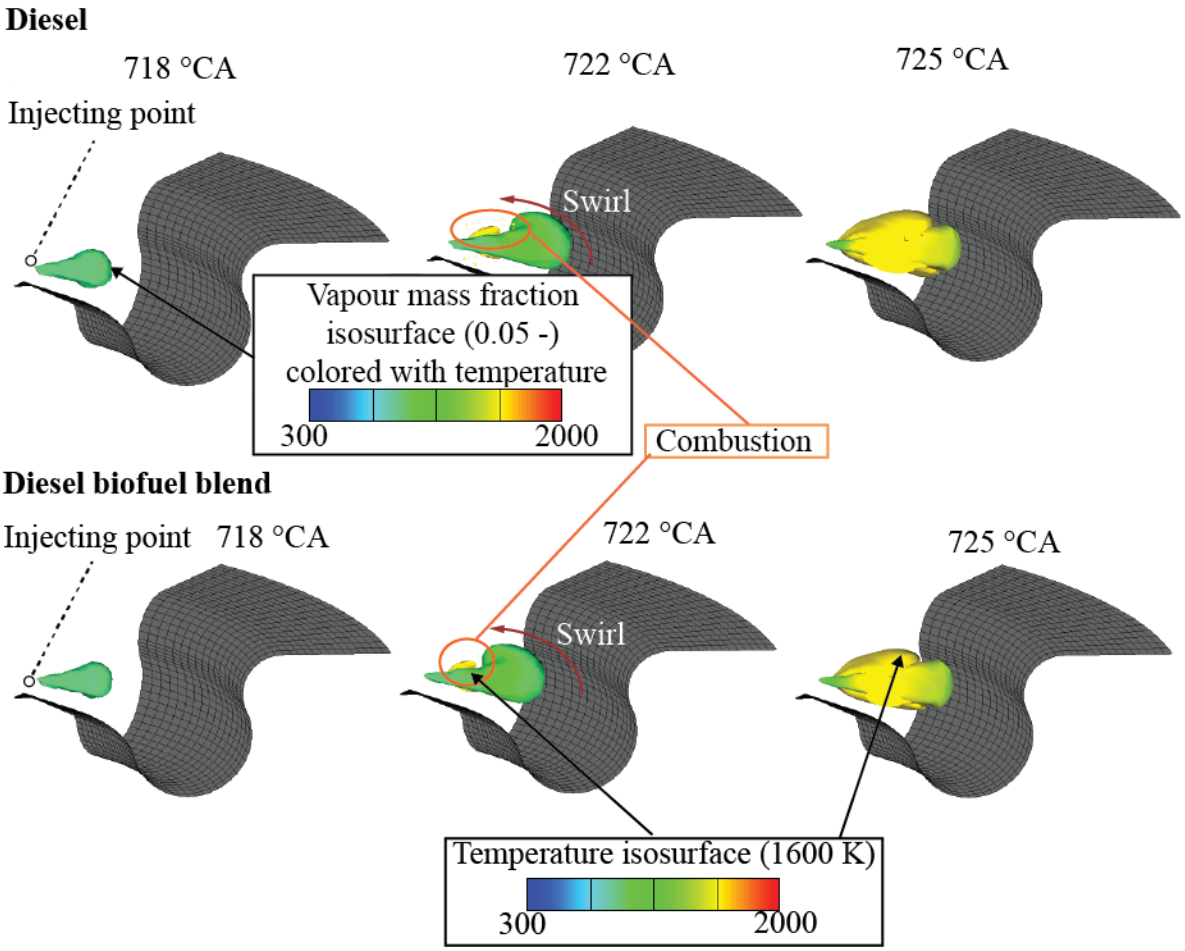

Figure 6 Comparison of calculated vapour fuel development at start of the combustion process

In observed modelling cases, adding the 7% of biofuel to create a mixture with diesel result in a reduction of the overall NO emissions. Figure 7 shows the isosurfaces of the NO species, high-temperature regions and the vapour cloud at the developed spray state – 727 °CA. At this crank angle position, the liquid fuel is evaporated and the vapour cloud is spreading through the domain. The vapour cloud is swirled and mixed with the hot environment which finally leads to the combustion process. The black isosurface presents the vapour cloud whilst the yellow one presents the high-temperature region where a temperature higher than 1600 K is noticed. When such high temperatures are achieved, the triple bond of nitrogen molecule are broken and thermal NO is formed. Both modelling cases exhibit a similar behaviour where a larger high-temperature region is noticed for pure diesel fuel combustion, which ultimately leads to faster NO species formation.

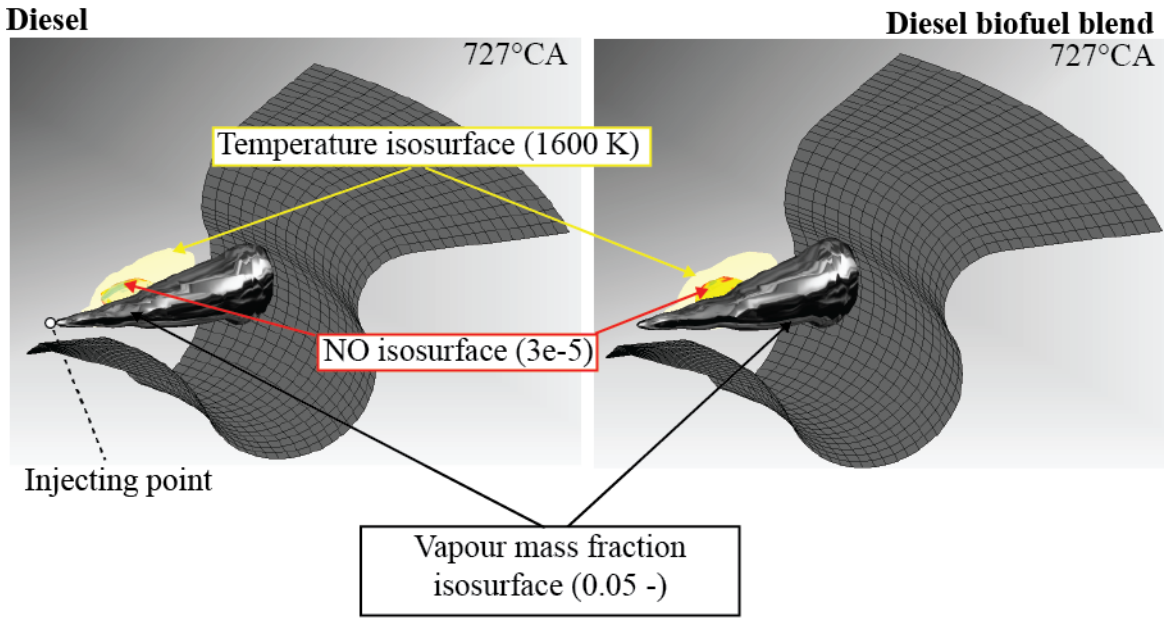

Figure 7 Comparison of calculated NO species at 727 °CA

6. CONCLUSION

Formation of pollutants during combustion in compression-ignition engines is a complex phenomenon depending on a range of parameters whose effect is hard to accurately estimate. Numerical modelling can serve as a valuable addition to the experimental investigations of different working conditions, geometries or fuel blends in the development of IC engines. This is especially true for the in-cylinder pollutant emission analysis, which is costly and problematic to observe in experimental setups, but of great interest when trying to optimise engine technologies to comply with the latest legislature.

Presented numerical model, implemented in the CFD code FIRE, covers all of the physics relevant to the pollutant emission. Spray, the effect of the flow field on it, as well as the disintegration of liquid fuel were modelled. Further, the process of fuel evaporation, ignition and combustion are included. Finally, the formation of emissions, both nitrogen-containing pollutants and the soot is covered by the model.

The model was validated by simulating the NO emissions over the range of operating conditions and comparing the data with experimental results. Furthermore, when biodiesel blend was used as a fuel, an average reduction in NO emissions of approximately 8% was found. This shows that a potential for the NO pollutant reduction in real IC engines exists, even with using biodiesel as fuel. Furthermore, these results indicate that the assumptions about the origin of the apparent increase of NO emissions in the experimental investigations might be correct, and that the differences in the operational parameters when comparing biodiesel blends and diesel could have caused the generally higher levels of NO for biodiesel. It can be concluded that under the identical conditions simulated in this work, biofuel powered IC engines produce less NO than the regular diesel ones. Further research should be directed at using detailed models for nitrogen-containing pollutant chemistry to obtain more accurate results for NO concentrations that could be used for the estimation of possible pollutant reduction when utilising biofuel blends.

ACKNOWLEDGEMENTS

The authors wish to thank the company AVL List GmbH, Graz, Austria for the financing and opportunity to work on the research project. Authors would also wish to thank the CFD Development group at AVL-AST, Graz, Austria, for their support.

REFERENCES

Baleta, J., Mikulčić, H., Vujanović, M., Petranović, Z., Duić, N., 2016. Numerical simulation of urea based selective non-catalytic reduction deNOx process for industrial applications. Energy Convers. Manag. 125, 59–69. doi:10.1016/j.enconman.2016.01.062

Cusidó, J.A., Cremades, L. V., 2012. Atomized sludges via spray-drying at low temperatures: An alternative to conventional wastewater treatment plants. J. Environ. Manage. 105, 61–65. doi:10.1016/j.jenvman.2012.03.053

Dukowicz, J., 1979. Quasi-steady droplet phase change in the presence of convection. Informal Rep. Los Alamos Sci. Lab. doi:10.2172/6012968

Dukowicz, J.K., 1980. A particle-fluid numerical model for liquid sprays. J. Comput. Phys. 35, 229–253. doi:10.1016/0021-9991(80)90087-X

Edelbauer, W., 2014. Coupling of 3D Eulerian and Lagrangian spray approaches in industrial combustion engine simulations. J. Energy Power Eng. 8, 190–200. doi:10.17265/1934-8975/2014.01.022

Energy Agency, I., 2015. CO2 Emissions From Fuel Combustion Highlights 2015.

Faeth, G.., Hsiang, L.-P., Wu, P.-K., 1995. Structure and breakup properties of sprays. Int. J. Multiph. Flow 21, 99–127. doi:10.1016/0301-9322(95)00059-7

Fenimore, C.P., 1971. Formation of nitric oxide in premixed hydrocarbon flames. Symp. Combust. 13, 373–380. doi:10.1016/S0082-0784(71)80040-1

FIRE manual 2013, 2013. . Graz.

Giakoumis, E.G., Rakopoulos, C.D., Dimaratos, A.M., Rakopoulos, D.C., 2012. Exhaust emissions of diesel engines operating under transient conditions with biodiesel fuel blends. Prog. Energy Combust. Sci. 38, 691–715. doi:10.1016/j.pecs.2012.05.002

Guan, B., Zhan, R., Lin, H., Huang, Z., 2015. Review of the state-of-the-art of exhaust particulate filter technology in internal combustion engines. J. Environ. Manage. doi:10.1016/j.jenvman.2015.02.027

Hanjalić, K., Popovac, M., Hadžiabdić, M., 2004. A robust near-wall elliptic-relaxation eddy-viscosity turbulence model for CFD. Int. J. Heat Fluid Flow 25, 1047–1051. doi:10.1016/j.ijheatfluidflow.2004.07.005

Hill, S.C., Smoot, L.D., 2000. Modeling of nitrogen oxides formation and destruction in combustion systems. Prog. Energy Combust. Sci. 26, 417–458. doi:10.1016/S0360-1285(00)00011-3

Katrašnik, T., 2007. Hybridization of powertrain and downsizing of IC engine – A way to reduce fuel consumption and pollutant emissions – Part 1. Energy Convers. Manag. 48, 1411–1423. doi:10.1016/j.enconman.2006.12.004

Khair, K.M., Majewski, W.A., 2006. Diesel Emissions and Their Control. SAE International.

Klemeš, J.J., Varbanov, P.S., Huisingh, D., 2012. Recent cleaner production advances in process monitoring and optimisation. J. Clean. Prod. 34, 1–8. doi:10.1016/j.jclepro.2012.04.026

Kozarac, D., Vuilleumier, D., Saxena, S., Dibble, R.W., 2014. Analysis of benefits of using

internal exhaust gas recirculation in biogas-fueled HCCI engines. Energy Convers. Manag. 87, 1186–1194. doi:10.1016/j.enconman.2014.04.085
Lapuerta, M., Armas, O., Rodríguez-Fernández, J., 2008. Effect of biodiesel fuels on diesel engine emissions. Prog. Energy Combust. Sci. 34, 198–223. doi:10.1016/j.pecs.2007.07.001
Martin Sommerfeld, Berend van Wachem, R.O. (Ed.), 2008. Best Practice Guidelines for Computational Fluid Dynamics of Dispersed Multiphase Flows.
Mikulčić, H., von Berg, E., Vujanović, M., Wang, X., Tan, H., Duić, N., 2016. Numerical evaluation of different pulverized coal and solid recovered fuel co-firing modes inside a large-scale cement calciner. Appl. Energy 184, 1292–1305. doi:10.1016/j.apenergy.2016.05.012
Miller, J.A., Bowman, C.T., 1989. Mechanism and modeling of nitrogen chemistry in combustion. Prog. Energy Combust. Sci. 15, 287–338. doi:10.1016/0360-1285(89)90017-8
Mobasheri, R., Peng, Z., Mirsalim, S.M., 2012. Analysis the effect of advanced injection strategies on engine performance and pollutant emissions in a heavy duty DI-diesel engine by CFD modeling. Int. J. Heat Fluid Flow 33, 59–69. doi:10.1016/j.ijheatfluidflow.2011.10.004
Naber, J., Reitz, R.D., 1988. Modeling Engine Spray/Wall Impingement. doi:10.4271/880107
Niemisto, J., Saavalainen, P., Pongracz, E., Keiski, R.L., 2013. Biobutanol as a Potential Sustainable Biofuel - Assessment of Lignocellulosic and Waste-based Feedstocks. J. Sustain. Dev. Energy, Water Environ. Syst. 1, 58–77.
Nordin, N., 2001. Complex Chemistry Modeling of Diesel Spray Combustion, CTH. Chalmers University of Technology.
O'Rourke, P.J., 1989. Statistical properties and numerical implementation of a model for droplet dispersion in a turbulent gas. J. Comput. Phys. 83, 345–360. doi:10.1016/0021-9991(89)90123-X
Petranović, Z., Edelbauer, W., Vujanović, M., Duić, N., 2017. Modelling of spray and combustion processes by using the Eulerian multiphase approach and detailed chemical kinetics. Fuel 191, 25–35. doi:10.1016/j.fuel.2016.11.051
Petranović, Z., Vujanović, M., Duić, N., 2015. Towards a more sustainable transport sector by numerically simulating fuel spray and pollutant formation in diesel engines. J. Clean. Prod. 88, 272–279. doi:10.1016/j.jclepro.2014.09.004
Reitz, R.D., 1987. Modeling atomization processes in high-pressure vaporizing sprays. At. Spray Technol. 3, 309–337.
Scheffknecht, G., Al-Makhadmeh, L., Schnell, U., Maier, J., 2011. Oxy-fuel coal combustion-A review of the current state-of-the-art. Int. J. Greenh. Gas Control 5, 16–35. doi:10.1016/j.ijggc.2011.05.020
Schiller, L., Naumann, Z., 1933. A drag coefficient correlation. Z.Ver.Deutsch.Ing 77, 318–320. doi:10.1016/j.ijheatmasstransfer.2009.02.006
Sun, J., Caton, J.A., Jacobs, T.J., 2010. Oxides of nitrogen emissions from biodiesel-fuelled diesel engines. Prog. Energy Combust. Sci. 36, 677–695. doi:10.1016/j.pecs.2010.02.004
Tashtoush, G.M., Al-Widyan, M.I., Albatayneh, A.M., 2007. Factorial analysis of diesel engine performance using different types of biofuels. J. Environ. Manage. 84, 401–411. doi:10.1016/j.jenvman.2006.06.017
Vallet, A., Burluka, A.A., Borghi, R., 2001. Development of a Eulerian Model for the "Atomization" of a Liquid Jet. At. Sprays 11, 24. doi:10.1615/AtomizSpr.v11.i6.20
von Berg, E., Edelbauer, W., Alajbegovic, A., Tatschl, R., Volmajer, M., Kegl, B., Ganippa, L.C., 2005. Coupled Simulations of Nozzle Flow, Primary Fuel Jet Breakup, and Spray Formation. J. Eng. Gas Turbines Power 127, 897. doi:10.1115/1.1914803

Vujanović, M., 2010. Numerical modelling of multiphase flow in combustion of liquid fuel. Fakultet strojarstva i brodogradnje, Sveučilište u Zagrebu.

Vujanović, M., Duić, N., Tatschl, R., 2009. Validation of reduced mechanisms for nitrogen chemistry in numerical simulation of a turbulent non-premixed flame. React. Kinet. Catal. Lett. 96, 125–138. doi:10.1007/s11144-009-5463-2

Vujanović, M., Petranović, Z., Edelbauer, W., Duić, N., 2016. Modelling spray and combustion processes in diesel engine by using the coupled Eulerian–Eulerian and Eulerian–Lagrangian method. Energy Convers. Manag. doi:10.1016/j.enconman.2016.03.072

Zeldovich, Y.A., Frank-Kamenetskii, D., Sadovnikov, P., 1947. Oxidation of nitrogen in combustion. Publishing House of the Acad of Sciences of USSR.

MODELLING POLLUTANT EMISSIONS IN DIESEL ENGINES, INFLUENCE OF BIOFUEL ON POLLUTANT FORMATION

Zvonimir Petranović*, Tibor, Bešenić, Milan Vujanović, Neven Duić

Faculty of Mechanical Engineering and Naval Architecture
University of Zagreb, Ivana Lučića 5, Zagreb, Croatia
e–mail: zvonimir.petranovic@fsb.hr, tibor.besenic@fsb.hr, milan.vujanovic@fsb.hr, neven.duic@fsb.hr

ABSTRACT

In order to reduce the harmful effect on the environment, European Union allowed using the biofuel blends as fuel for the internal combustion engines. Experimental studies have been carried on, dealing with the biodiesel influence on the emission concentrations, showing inconclusive results. In this paper numerical model for pollutant prediction in internal combustion engines is presented. It describes the processes leading towards the pollutant emissions, such as spray particles model, fuel disintegration and evaporation model, combustion and the chemical model for pollutant formation. Presented numerical model, implemented in proprietary software FIRE®, is able to capture chemical phenomena and to predict pollutant emission concentration trends. Using the presented model, numerical simulations of the diesel fuelled internal combustion engine have been performed, with the results validated against the experimental data. Additionally, biodiesel has been used as fuel and the levels of pollutant emissions have been compared to the diesel case. Results have shown that the biodiesel blends release lower nitrogen oxide emissions than the engines powered with the regular diesel.

Keywords: Diesel engine; Biodiesel, Combustion; Spray process; CFD

1. INTRODUCTION

During operation of Internal Combustion (IC) diesel engines a vast amount of fossil fuel is consumed, and therefore they represent a threat to the environment in terms of pollutant emissions. In theoretical conditions, when the complete fuel combustion is achieved, solely the CO_2 and H_2O species would be generated. However, such conditions are impossible to achieve due to the engine transient operating conditions. In 2013, 25% of the global CO_2 emissions originated from the transportation sector (Energy Agency, 2015). In addition, as a consequence of IC engine operating conditions, several other species, such as CO, HC, PM and NO_x, are produced. Relative to the total flue gases flow, 1% belong to these species, of which approximately 50% are the NO_x species (Khair and Majewski, 2006).

As a part of the tendency towards cleaner transport sector with lower impact on the environment, concentrations of the emitted pollutant emissions have been regulated in the past decade (Klemeš et al., 2012), and more stringent conditions are enforced by the governmental policies every year. Comparing to the spark ignition engines, the diesel engines are characterised by greater energy conversion and safety factor (Katrašnik, 2007). In order to remain the most used vehicle powering source on the European market, as well as to meet the higher efficiency standards, the IC engines efficiency must be constantly improved (Kozarac et al., 2014). In addition to the emission

regulations, another obstacle for IC engine utilisation is the promotion of biofuels in the transportation sector (Niemisto et al., 2013). As a part of the European biofuels directive (2003/30/EC) in 2003, a minimum level of used biofuels was enforced to all EU member states. Recently, the European Standards Committee (CEN) allowed the maximum amount of bio – content up to 7%, and even a higher values are expected in the near future. Biodiesel is derived by transesterification, does not contain sulphur, degrades quickly, and is nontoxic (Tashtoush et al., 2007). In addition to the engine performance optimisation, NO emissions can be reduced by introducing various exhaust gas recirculation and engine boosting systems. A good review regarding exhaust particle filter technologies is shown in (Guan et al., 2015).

The combustion process within the IC diesel engine can be divided into two distinguished parts: the uncontrollable premixed combustion which takes place during the autoignition process, and mixing-controlled diffusion combustion. Most of the vaporised fuel is combusted in the diffusion regime and therefore the overall engine efficiency highly depends on the spray process. The spray is a highly transient and turbulent multiphase process, which consists of several distinguished processes, such as fuel jet disintegration, droplet atomization and collision, an evaporation process, air entrainment, etc.

Spray is a versatile process, apart from the internal combustion engines also used in removing pollutant emissions (Baleta et al., 2016), and the numerous experimental investigations have been performed. However, with the progress of computational power and development of Computational Fluid Dynamic (CFD) tools, combining experimental research with CFD analysis became the common approach. With such approach, an understanding of complex and transient turbulent flows that are hard to capture experimentally can be significantly improved. For the reliable use of CFD tools, each of the used submodels should be previously validated. Finally, combining the CFD tools with experimental research could result in a reduction of the overall expenses and investigation duration.

There are various approaches developed for the computational modelling of turbulent dispersed multiphase flows, such as Direct Numerical Simulation (DNS) for the particles, the Discrete Particle Model (DPM), the Euler-Lagrangian (EL), and the Euler Eulerian (EE) model, etc. (Martin Sommerfeld, Berend van Wachem, 2008). The EL approach is the most used approach for modelling the spray process. While it suffers from several disadvantages, such as mesh dependency, parallel calculation efficiency reduction, high particle loading (Petranović et al., 2015), the EL approach is sufficiently accurate and efficient for modelling the diluted spray region, as shown for the liquids by Faeth et al. (Faeth et al., 1995), as well as for solid particles (Mikulčić et al., 2016). In order to overcome its disadvantages, the EE approach can be used (Vujanović et al., 2016)(Petranović et al., 2017). Within EE approach both the liquid and the gas phases are treated as a continuum. For improved accuracy, the discrete phase is sorted into a finite number of classes, characterised by the mean droplet diameter (FIRE manual 2013, 2013). The phase interaction is achieved through source terms in the conservation equations accounting for the droplet dynamics. Despite the increased computational power requirements compared to the EL approach, the EE approach is suitable for modelling all spray regimes, including the dense spray region.

To overcome disadvantages inherent to the EL and the EE approaches, they can be coupled by using the AVL FIRE® Code Coupling Interface (ACCI) (von Berg et al., 2005)(Edelbauer,

2014)(Vujanović et al., 2016) or through the ELSA modelling concept (Vallet et al., 2001). The difference between these modelling concepts is that in the ACCI approach, the gas and the liquid phases in the vicinity of the nozzle are treated separately, and within the ELSA model they are treated as one mixture phase.

Available literature on usage of biodiesel blends as fuel in compression-ignition engines generally reports decrease in particulate matter (PM), hydrocarbon (HC) and carbon monoxide (CO) emissions as benefits, as well as increased levels of NO_x emissions as one of the main drawbacks of biodiesel implementation (Giakoumis et al., 2012). However, a deeper insight into reported experimental results questions this increasing trend and analyses its causes. For example, a comprehensive literature review (Lapuerta et al., 2008) examines differences in fuel injection and combustion due to disparities in physical and chemical properties of biodiesel, such as lower heating value, bulk modulus and viscosity etc. It is similarly (Sun et al., 2010) concluded that, although the increase in NO_x production exists, it is not inherent to the biofuel itself, but rather due to the usage of biodiesel in unmodified diesel engine setups. This way, the difference in biodiesel properties advances the start of injection process and increases the combustion temperatures, leading to the elevated NO_x emissions. In real-life experimental setups, it is often hard to ensure consistent operational parameters when comparing different fuels (e.g. the same start and the end of injection). In these situations, numerical simulations can be a great tool for analysis and comparison of performances of different fuels in the same working regimes.

It is one of this papers' aims to numerically investigate the NO_x pollutant emissions when using biodiesel blends, compared to the identical conditions with regular diesel fuel. Therefore, it is important to understand the thermochemical phenomena behind the formation of NO_x. Nitrogen-containing emissions from the combustion processes are commonly classified as thermal, prompt, and fuel NO_x, relative to the mechanism of their production (Vujanović, 2010). Thermal NO_x forms by dissociation of the molecular nitrogen from the air and is highly temperature-dependent, prompt NO_x occurs in nitrogen reactions with hydrocarbon radicals in the first stages of reactions, and the fuel NO_x is formed by complex reaction paths from nitrogen contained in the fuel. In modern CFD approaches, NO_x emissions are almost invariantly modelled as a post-processing step after calculation of the flow field and main combustion. This is justified by the, in absolute terms, small concentrations of NOx, which have a low impact on overall flow field, temperature and concentrations of major combustion products, as well as by different time scales of the fast combustion reactions and the relatively slower production of NO_x (Hill and Smoot, 2000). Although detailed kinetic mechanisms exist (Miller and Bowman, 1989), in order to obtain the computationally efficient model, some simplifications need to be made. Chemical model simplifications, such as omitting the species with negligible concentrations, removing reaction paths with minute influence on the overall NO_x production or the assumption of chemical equilibrium are a common approach to simplifying complex chemical phenomena for usage in CFD. Reduced number of chemical equations allows for an efficient coupling with the turbulent reacting flow. Chemistry-turbulence interaction was modelled by taking into the account temperature fluctuations, integrating the chemical reaction rates and applying the Probability Density Function (PDF) approach (Vujanović et al., 2009). Presented numerical model for modelling NO_x emissions has been implemented in the CFD code FIRE.

The paper is structured as follows: first, the description of the available experimental data is given. Later, the short introduction into the Euler-Lagrangian spray modelling is provided, together with

the NO_x modelling equations. Afterwards, the numerical setup is described and the results are thoroughly discussed. Finally, the conclusions are drawn in section 'Conclusions'.

2. AVAILABLE EXPERIMENTAL DATA

To find the most suitable NO_x modelling approach, the single cylinder engine was computationally modelled. This engine is designed as a Single CYlinder ENgine (SCYLEN), with electro-hydraulic valve actuation, and the ω-shaped piston. The main SCYLEN engine and injector system characteristics are shown in Table 1.

Table 4 Engine specifications

Bore (mm)	85	**Spray Angle (°)**	158
Stroke (mm)	94	**Displacement (mm^3)**	533.4
Compression ratio (-)	16:1	**Nozzle (-)**	8-hole
Nozzle location (mm)	2,0,-3.8	**Inj. Pressure (bar)**	1200-1600
Orifice diameter (mm)	0.1		

For the research purposes several engine operating points were examined, and the main combustion parameters are shown in Table 2.

Table 5 Engine combustion parameters

Case	SOI – EOI (°CA)	Swirl (1/min)	Injected mass (kg)	EGR mass fraction (%)
a	712.5 – 735.4	5832	3.37×10^{-6}	23.84
b	713.5 – 734.4	5544.6	3.41×10^{-6}	19.68
c	712.5 – 735.4	5832	3.37×10^{-6}	23.84
d	712.5 – 733.4	4030.2	3.4×10^{-6}	23.5
e	713.4 – 736.1	4048.2	3.38×10^{-6}	23.36
f	714.4 – 736.9	4072.8	3.38×10^{-6}	16.16

Table 3 shows the measured NO_x and soot emission concentrations expressed per kilogramme of exhaust gases measured at the time of exhaust valve opening. The pressure measurements have been carried out using the PUMA Open system, whilst the pollutant emissions have been measured using the AVL emission measurement system.

Table 6 Measured emission concentrations

Case	Soot (kg/kg)	NO (kg/kg)	Case	Soot (kg/kg)	NO (kg/kg)
a	2.09×10^{-5}	5.62×10^{-4}	d	2.50×10^{-5}	4.33×10^{-4}
b	1.67×10^{-5}	5.55×10^{-4}	e	5.28×10^{-5}	3.43×10^{-4}
c	6.64×10^{-5}	3.64×10^{-4}	f	1.92×10^{-5}	5.60×10^{-4}

3. NUMERICAL MODEL

To calculate the spray process occurring inside the IC engine combustion chamber the EL approach was used. In such approach, the gas phase is treated as the continuous phase in the Eulerian framework, whilst the Lagrangian formulation is used to describe the discrete phase dynamics. In the Lagrangian formulation samples of individual droplets with the same physical properties and dimensions are tracked through the domain. These samples are commonly known as parcels (Dukowicz, 1980). The grouping procedure, in comparison to tracking each fuel droplet, reduces the overall computational effort. Following expression is used to calculate parcel trajectory:

$$\rho_l \frac{du_P}{dt} = \sum F , \tag{1}$$

where the terms on the left-hand side are the density and the parcel acceleration, whilst the term on the right-hand side represents the forces acting on the droplet parcel *P*. The force term may get its contribution from drag, gravity, buoyancy, pressure difference, and external forces. In the observed application, the main force that results in droplet momentum dissipation is the drag force.

3.1. Spray submodels

By injecting the liquid fuel with high velocity through small diameter nozzle holes, fuel is subject to the atomization process. The atomization is driven by the occurrence of the surface instabilities which are a consequence of the aerodynamic and turbulent forces. As a result, a population of small diameter droplets is distributed within the combustion chamber, which is later evaporated and combusted. Next sections show brief introduction into models utilised for a description of the spray process.

3.1.1. Fuel disintegration

Liquid sprays are used in various technical applications, such as internal combustion engines, gas turbines, spray painting, spray cooling, fire extinction, waste treatment, spray quenching, spray drying (Cusidó and Cremades, 2012), etc. In this research, the liquid fuel was injected through the high-pressure injection systems that generate high-velocity fluid motion, and therefore we employed the WAVE disintegration model. The used WAVE disintegration model considers the occurrence of surface instabilities due to the Kelvin-Helmholtz (KH) and Rayleigh-Taylor (RT) instabilities. The RT instabilities are a result of the acceleration of dense medium by the less dense one, whilst KH instabilities are a result of shear forces acting on the droplet surface. To match experimental data, the WAVE model offers two distinguished modelling constants, where one constant is correlating the diameter of created droplet with the wavelength of the fastest surface instability, and other is used to correct the breakup time, according to next equations:

$$r_{stable} = B_0 \Lambda \tag{2}$$

$$\tau_a = 3.726 B_1 \frac{r_k}{\Lambda_k \Omega_k} , \tag{3}$$

where r_{stable} is the target diameter, B_0 is the modelling constant, Λ is the wavelength of the surface instability, τ_a is the atomization time scale, B_1 is the modelling constant, r_k is the droplet diameter, and Ω is the surface instability growth rate. The Λ and Ω are in a function on local flow properties and they are calculated by using the semi empirical (Reitz, 1987):

$$\Lambda_k = 9.02 r_k \frac{\left(1+0.45\cdot Oh^{0.5}\right)\left(1+0.4\cdot T^{0.7}\right)}{\left(1+0.87\cdot We_1^{1.67}\right)^{0.6}} \tag{4}$$

$$\Omega_k = \left(\frac{\rho_k {r_k}^3}{\sigma}\right)^{-0.5} \frac{0.34+0.38\cdot We_1^{1.5}}{\left(1+Oh\right)\left(1+1.4\cdot T^{0.6}\right)}, \tag{5}$$

where Oh is is the Ohnesorge number, T is the Taylor number, and We_1 is the gas phase Weber number. The mass loss due to the atomization process is shown with next equation:

$$\frac{dm_k}{dt} = 4\pi {r_k}^2 \rho_k \frac{dr_k}{dt}\ , \tag{6}$$

where term on the left side of the equation is the mass loss of class k, ρ_k is the fuel density and last term is the artificial diameter reduction defined as:

$$\frac{dr_k}{dt} = -\frac{r_k - r_{\text{target}}}{\tau_A},\ r_{\text{target}} \le r_k\ . \tag{7}$$

3.1.2. Fuel evaporation

In this research, the Dukowicz evaporation model was employed to predict the discrete phase heating and evaporation (Dukowicz, 1979). This model assumes that the droplet is spherical in shape and a steady quasi-film is present around the droplet surface. The droplet has infinite conductivity, uniform physical properties are assumed in the surrounding gas, and the thermal equilibrium is assumed on the droplet surface. The disadvantage of the Dukowicz evaporation formulation is that it is suitable for predicting evaporation when the ratio of thermal diffusivity to mass diffusivity is equal to unity and that it is not capable of predicting the condensation of the gas species. However, for the observed application, this model is capable of predicting the evaporation process, which will be shown in the result section.

3.1.3. Momentum exchange

As it was previously mentioned, the drag force is the main contributor to momentum exchange between the continuous and the discrete phase. The drag force is calculated according to the following expression:

$$F_D = \frac{\rho_g}{2} c_D A_D {u_{rel}}^2, \tag{8}$$

where ρ_g is gas phase density, term c_D is the drag coefficient, A_D is projected area, and u_{rel} the gas-liquid relative velocity. To model the drag coefficient of a single sphere, in this research the following formulation was used (Schiller and Naumann, 1933):

$$c_D = \begin{Bmatrix} \frac{24}{\mathrm{Re}}\left(1+0.15\cdot \mathrm{Re}^{0.687}\right) \rightarrow \ for\ \mathrm{Re} \le 1000 \\ 0.44 \rightarrow \ for\ \mathrm{Re} > 1000 \end{Bmatrix}. \quad (9)$$

3.1.4. Spray-wall interaction

In operation of diesel engines, the spray-wall interaction may have a significant role, especially for small bore engines where the distance between injector and piston surface is small. To take into account the droplet behaviour after a collision with the piston surface, approaches such as the wall interaction model or the wall film physics can be employed. In this research, the authors utilised the wall film module where parcel rebound/reflection is modelled depending on the Weber number (Naber and Reitz, 1988).

3.1.5. Droplet collision

From the viewpoint of the statistical particle method, which is the basis of the EL spray approach, the droplet collision process is modelled by a statistical approach. The most common approach is the O'Rourke collision model (O'Rourke, 1989), which has disadvantages such as mesh dependency. To overcome mesh dependency disadvantage, we employed the approach developed by Nordin (Nordin, 2001), which is an improvement of the O'Rourke approach (*FIRE manual 2013*, 2013).

3.2. The pollutant formation model

3.2.1. The NO_x model

Significant amounts of nitrogen-containing pollutants are emitted in the environment with the combustion of diesel fuels. Nitrogen oxides is the collective term for the family of seven polluting chemical compounds: nitrogen monoxide (NO), nitrogen dioxide (NO_2), nitrous oxide (N_2O), dinitrogen dioxide (N_2O_2), dinitrogen trioxide (N_2O_3), dinitrogen tetroxide (N_2O_4) and dinitrogen pentoxide (N_2O_5) (Vujanović, 2010). Diesel combustion releases NO_x emissions predominantly as NO, with levels of other nitrogen species in the negligible amounts (Scheffknecht et al., 2011). Therefore, all of the NO_x emissions are modelled as NO. For tracking the NO species concentrations, transport equation above was solved.

$$\frac{\partial(\bar{\rho}\tilde{Y}_{\mathrm{NO}})}{\partial t} + \frac{\partial(\tilde{u}_i \bar{\rho}\tilde{Y}_{\mathrm{NO}})}{\partial x_i} = \frac{\partial}{\partial x_i}\left(\bar{\rho} D_t \frac{\partial \tilde{Y}_{\mathrm{NO}}}{\partial x_i}\right) + \bar{S}_{\mathrm{NO}}. \quad (10)$$

On the left-hand side, the first term describes the temporal change of the NO concentrations, and the second one shows convection change. On the right-hand side, the first term describes the diffusive change, while the last term stands for the source of NO. Generally, the aforementioned nitrogen oxides formation mechanisms together comprise the NO source term, as seen in Eq. (11). Thermal mechanism forms nitrogen oxides in post-flame regions by oxidation of nitrogen, prompt NO is formed in reactions of molecular nitrogen with hydrocarbon radicals, and the fuel NO occurs as the result of the several parallel reaction paths from the fuel contained nitrogen. However, in compression-ignition engine applications fuel NO is considered irrelevant (Mobasheri et al., 2012). Thus, the source term S_{NO} is comprised only of the most influential reaction mechanisms –

the thermal and the prompt NO – and third term in Eq. (11) equals zero. Terms inside the brackets stand for the temporal concentration changes for thermal, prompt and fuel NO respectively, and M_{NO} is the NO molar mass.

$$S_{NO} = M_{NO}\left(\frac{dc_{NOthermal}}{dt} + \frac{dc_{NOprompt}}{dt} + \frac{dc_{NOfuel}}{dt}\right) \tag{11}$$

Thermal NO concentrations are highly influenced by the local temperature. The strong triple covalent bonds of the molecular nitrogen from the air have high activation energy that needs to be exceeded for the reaction to proceed. For this reason, dissociation of nitrogen is considered to be the rate-limiting step of the thermal reaction mechanism. Another parameter that thermal NO depends greatly upon is the concentration of the O and OH radicals. Reported numerical models almost invariantly use three chemical equations of the extended Zeldovich mechanism (Zeldovich et al., 1947) for modelling the thermal NO emissions. Reaction in Eq. (12) describes dissociation of the molecular nitrogen contained in the air by the oxygen radicals. Nitrogen produced this way is oxidised (Eq. 13) and further reacts with the OH radicals that can have high concentrations in fuel-rich conditions (Eq. 14).

$$\mathrm{N_2} + O \overset{k_1}{\leftrightarrow} \mathrm{NO{+}N} \tag{12}$$

$$\mathrm{N} + \mathrm{O_2} \overset{k_2}{\leftrightarrow} \mathrm{NO{+}O} \tag{13}$$

$$\mathrm{N} + \mathrm{OH} \overset{k_3}{\leftrightarrow} \mathrm{NO} + \mathrm{H} \tag{14}$$

Both forward and backwards chemical reaction rate coefficients for above three equations are modelled according to the Arrhenius law. Further model simplification is the assumption of the quasi-steady-state for the nitrogen atoms. This way atomic nitrogen is consumed as fast as it is produced, and the overall thermal NO source can be simplified (*FIRE manual 2013*, 2013).
Contrary to the slower and temperature-dependent thermal NO formation, prompt NO – firstly described by the Fenimore (Fenimore, 1971) – forms earlier by the fast reactions of nitrogen in the fuel-rich regions. In the combustion process fuel is fragmented into the hydrocarbon radicals, denoted by the overall formula CH_i, that react with nitrogen and form hydrogen cyanide (HCN). HCN then participates in a series of rapid reactions and is subsequently oxidised to produce NO (Petranović et al., 2015).

$$\mathrm{CH}_i + \mathrm{N_2} \longleftrightarrow \mathrm{HCN} + \mathrm{N} + \cdots \tag{15}$$

Overall prompt NO is described by the expression in Eq. (16), which provides improved results by including the correction factor obtained from comparison with experimental data (Vujanović, 2010).

$$\frac{dc_{NO}}{dt} = k\ f{c_{O_2}}^{b} c_{N_2} c_{fuel} \exp\left(-\frac{E}{RT}\right) \tag{16}$$

The impact of the turbulent fluctuations of temperature and species concentrations on NO production is highly nonlinear. Their effect is taken into account by considering Probability Density Function (PDF). PDF is assumed to be a two-moment beta function, as appropriate for combustion calculations. It is defined as in Eq. (17.), with B being the beta function, and the α and β being functions of the mean temperature and its variance, obtained by solving transport equation for variance of temperature (Vujanović, 2010):

$$P(T) = \frac{T^{\alpha-1}(1-T)^{\beta-1}}{B(\alpha,\beta)} = \frac{\Gamma(\alpha+\beta)}{\Gamma(\alpha)\Gamma(\beta)} T^{\alpha-1}(1-T)^{\beta-1}. \tag{17}$$

Gamma function Γ is defined according to the following:

$$\Gamma(z) = \int_0^\infty e^{-t} t^{z-1} dT. \tag{18}$$

Finally, the mean turbulent rate of production of NO is obtained by Eq. (19), where $S_{Y_{NO}}$ is the integrated instantaneous rate of production.

$$\overline{S}_{Y_{NO}} = \int_0^1 P(T) S_{Y_{NO}}(T) dT \tag{19}$$

3.2.2. The soot model

At high temperatures and fuel-rich conditions, hydrocarbon fuels show the tendency to form carbonaceous particles, otherwise known as soot. The soot is formed in the early stage of the engine working cycle, but it is later oxidised. To model the soot formation rate, the transport equation for the soot mass fraction is solved. In this work, the Kinetic soot model characterised with a reduced number of species and reactions was employed. The basis of used soot model is a soot chemical reaction mechanism that covers approximately 1850 homogeneous reactions, 186 species and 100 heterogeneous reactions (*FIRE manual 2013*, 2013).

4. CALCULATION SETTINGS AND NUMERICAL SETUP

Spray process was modelled by using the EL spray modelling approach, whilst the combustion process was modelled by employing the common ECFM-3Z combustion model (*FIRE manual 2013*, 2013). Such model is a reasonable choice in modelling the IC Diesel engine since it correctly describes both the premixed and diffusion flames. Several engine operating points were simulated, as shown in Table 2 and Table 3. The detailed information on the nozzle flow conditions was not known and authors assumed non-cavitating symmetrical nozzle flow conditions. Therefore, the CFD simulations were performed on engine segment mesh covering 1/8 (45°) of the cylinder bowl and one nozzle hole, as can be seen in Figure 1. With aforementioned assumption, the CPU costs were significantly reduced.

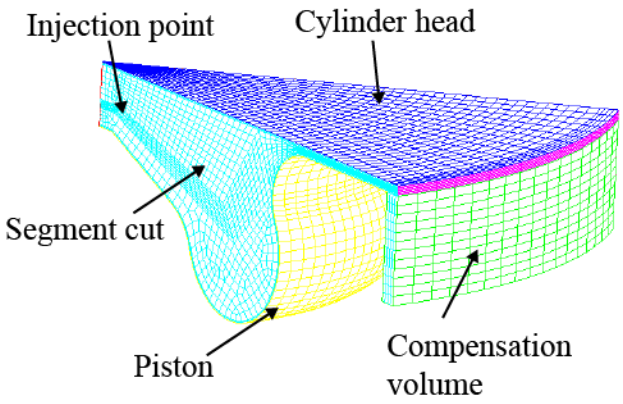

Figure 8 Generated computational mesh with defined selections

The liquid fuel was injected from the certain point of the computational domain in the direction defined by the nozzle geometry, as defined in Table 1. For all operating conditions, the cylinder head and piston selection were defined as non-permeable wall boundary conditions with a constant temperature of 500 and 550 K, respectively. To achieve the real engine compression ratio, compensation volume selection had to be generated since the computational domain was simplified, comparing to the real chamber geometry. Only one segment of the whole chamber was modelled and therefore the periodic boundary condition was applied to the segment cut selection. The generated computational mesh contains approximately 23800 control volumes in the Top Dead Centre (TDC) and 67500 control volumes in the Bottom Dead Centre (BDC). The piston selection was defined as moving mesh which resulted in deformation of certain computational cells. Therefore, the mesh was rezoned several times to satisfy predefined conditions of aspect ratio and cell orthogonality.

The Central Differencing Scheme (CDS) was used for discretization of the continuity equation, and the Upwind Differencing Scheme (UDS) was used for turbulence, energy and scalar transport equations. The blend between the CDS and UDS differencing schemes with blending factor of 0.5 was used for the momentum equations. The turbulence was modelled by using the advanced $k - \zeta - f$ turbulence model (Hanjalić et al., 2004). This model is robust enough and can be used for simulations with moving computational meshes and swirled compressed flows, as it is the case in the observed engineering application.

5. RESULTS AND DISCUSSION

The initial step of this research was to find the most suitable NO production mechanism for the observed IC engine configuration, and the results are shown in Figure 2. Around the TDC the local in-cylinder temperatures reach over 2000 K, which is high enough to break strong triple bonds of the N_2 species. Therefore, the thermal mechanism was employed on two different engine operating points and compared with the experimental data. The results of NO concentrations with only thermal NO mechanism are shown for operating points *a* and *b*, where rather big discrepancies with the experimental data are noticeable. To increase the accuracy of CFD simulations, production of NO species by the prompt mechanism was introduced. Characteristic for the prompt mechanism is that generation of NO occurs earlier than NO produced by the thermal mechanism, and it usually increases the overall NO concentrations. For both of the mentioned NO modelling approaches, the NO emissions are calculated from the mean or averaged quantities, which can be

improved by coupling the NO generation with the turbulence. Therefore, the effect of turbulence was introduced through the PDF of temperature variance which improved the prediction of absolute NO concentrations for all engine operating points.

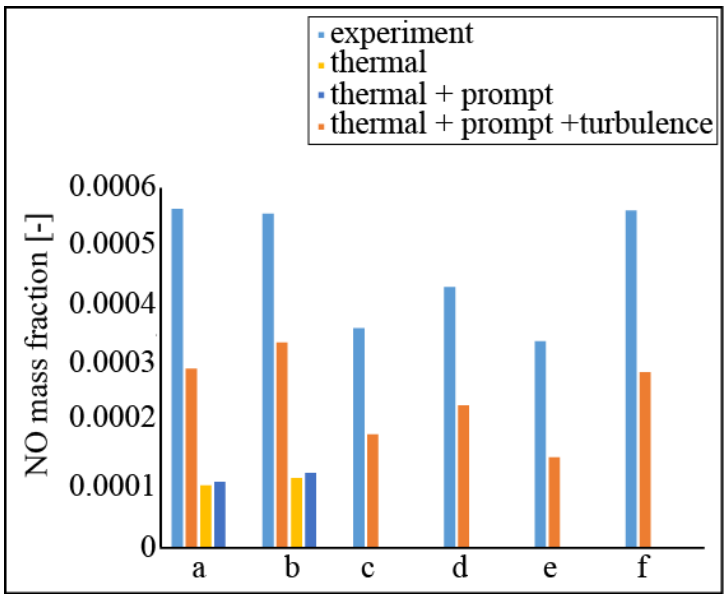

Figure 9 **NO_x concentrations for different modelling approaches compared with the experimental data**

For a correct prediction of the absolute NO emissions, a more detailed IC engine simulation should be performed. In presented modelling cases some simplifications exist that could have an impact on pollutant emission modelling. It is well known that NO prediction is influenced by:

- Nozzle flow conditions: the authors acquired the injection rate from the experimental research. This information could be improved by information such as mass flow distribution between nozzle holes, generation of vapour phase through the cavitation process, real inlet boundary conditions such as temperature, volume fractions of discrete and continuous phase, etc. It is known that nozzle flow can have a significant impact on the overall spray shape and thus, it can influence the fuel-air mixing, combustion, and pollutant formation.
- Spray shape: for more detailed results, quantities such as liquid and vapour penetrations should be acquired for spray parameterization. Also, information such as axial and radial mixture distribution, spray angle, droplet distribution, etc. would be beneficial. Aforementioned information should be acquired at least for one engine case, or for artificial constant volume case with similar parameters to tune the spray submodels. It is a known fact that in IC engine the combustion is mostly mixing-driven and therefore, spray plays a major role in predicting the temperature development, which finally dictates the NO generation and destruction rate.
- The used combustion model which is thoroughly validated on many applications could be replaced with detailed, skeletal or reduced chemistry mechanism.
- The boundary and the initial conditions that are taken from the experimental research as a mean value. This could be improved by simulating suction stroke where information such

as swirl number, turbulent kinetic energy and dissipation rate, etc. would be acquired for the whole engine cycle. Also, mesh topology could include the injector and valve heads volumes, which would lead to the removal of compensation volume shown in Figure 1.

Due to simplification of the engine model, it is more reasonable to track the trend of pollutant emissions. This implies that the relative change of NO and soot concentrations with engine operating conditions modification is of greater interest. The emission trends are shown in Figure 3, where a good agreement with the experimental data is achieved, both for the NO and soot emissions.

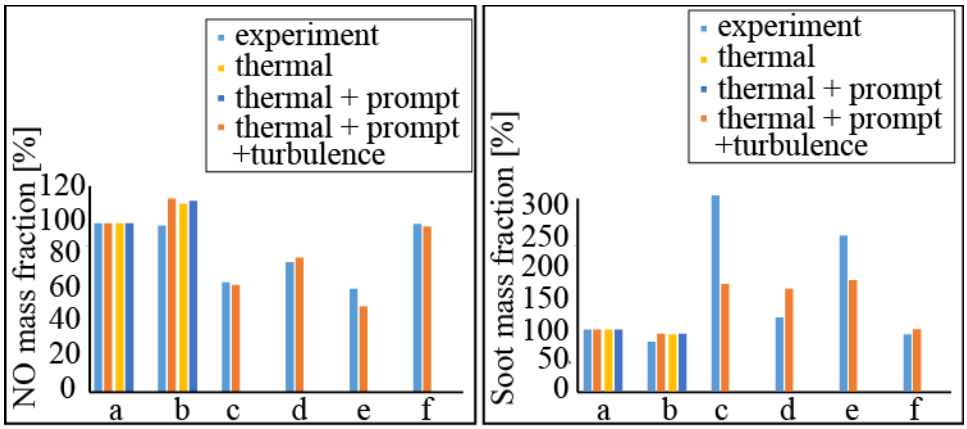

Figure 10 Normalised pollutant concentrations for different modelling approaches compared with the experimental data

In the last step of the research, diesel fuel was replaced with the EN590B7 mixture, which is a blend of diesel with 7% of fatty acid methyl esters (FAME), and performed the CFD simulations for all operating points. Here, the thermal and prompt NO mechanisms were employed, with the turbulence interactions included through the PDF function. The results of biodiesel addition for observed engine configuration are shown in Figure 4, where similar levels of NO concentrations were obtained for both fuels. The trend with changing engine operating conditions is the same for both fuels, but the biofuel addition exhibits lower values of absolute NO concentrations. The averaged decrease in predicted NO mass fraction with the addition of the biofuel is 8.02%.
These results differ from the greater part of the experimental data from the literature, where NO concentration increases are reported when using biodiesel. It should be noted, as was mentioned before, that experimental results were obtained by simply replacing the fuels and thus altering the start and the end of injection – considered the main culprit for the temperature change and the NO emission increase. In the present work, all of the simulation parameters were kept the same, which is crucial for the valid comparison of the results.

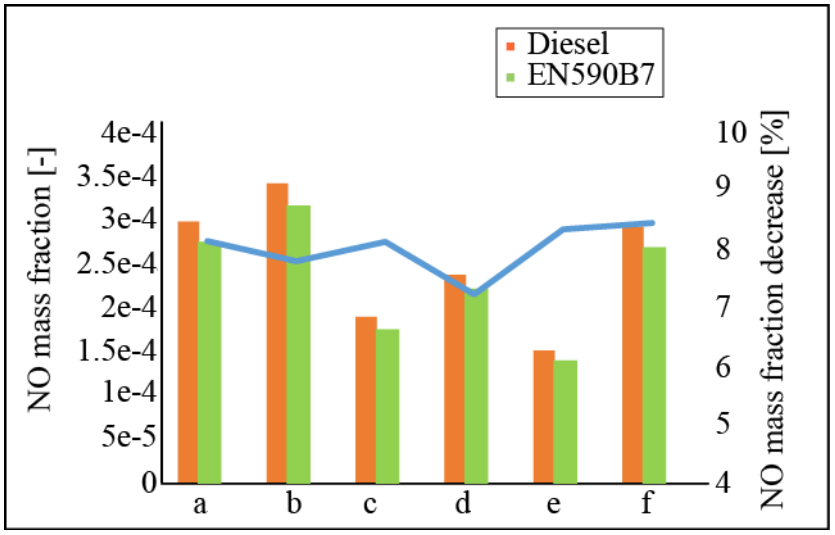

Figure 11 NO concentrations reduction due to biofuel addition

Figure 5 shows the mean pressure and temperature profiles for the engine compression and expansion strokes. It can be seen that the calculated results are in an excellent agreement with the measured data. The pressure and temperature rise due to a reduction in engine working volume in the compression stroke. At a certain crank angle position, few degrees before TDC, the liquid fuel is injected into the cylinder. The liquid fuel disintegrates into small diameter droplets and evaporates, which is visible in temperature reduction due to the heat consumed. After the fuel vapour is produced and mixed with the hot gas mixture, ignition starts and in-cylinder pressure and temperature rise rapidly. At 720° the piston moves towards BDC and the working volume is increased, leading to pressure and temperature reduction.

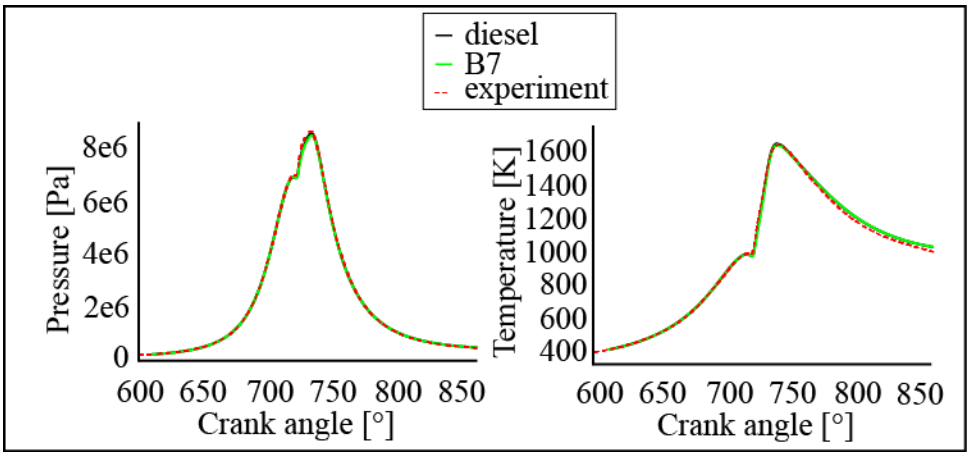

Figure 12 Mean pressure and temperature profiles

At later crank angle positions when a significant amount of vapour mass is produced and mixed with the hot surrounding gases, the exothermic chemical reactions occur. The release of heat through the chemical reactions – the combustion process, lead to a rapid temperature increase at a certain location within the combustion chamber. The combustion process starts at the periphery of the vapour cloud, as visible in Figure 6. This figure shows isosurface of vapour mass fraction coloured with the temperature of surrounding gas phase, and the isosurface representing the gas

phase temperature of at least 1600 K. The results obtained with the injection of diesel fuel and diesel biofuel blend shows similar occurrence of the combustion process around 722 °CA, and later flame consumes the vapour cloud towards the injector. The development of high-temperature contour is visible at crank positioned at 725 °CA. In the conducted simulations, the combustion process occurs slightly earlier and it is more pronounced in the case of pure diesel fuel combustion. A more progressive combustion process leads to higher local in – cylinder temperatures, and thus higher concentrations of pollutant NO species.

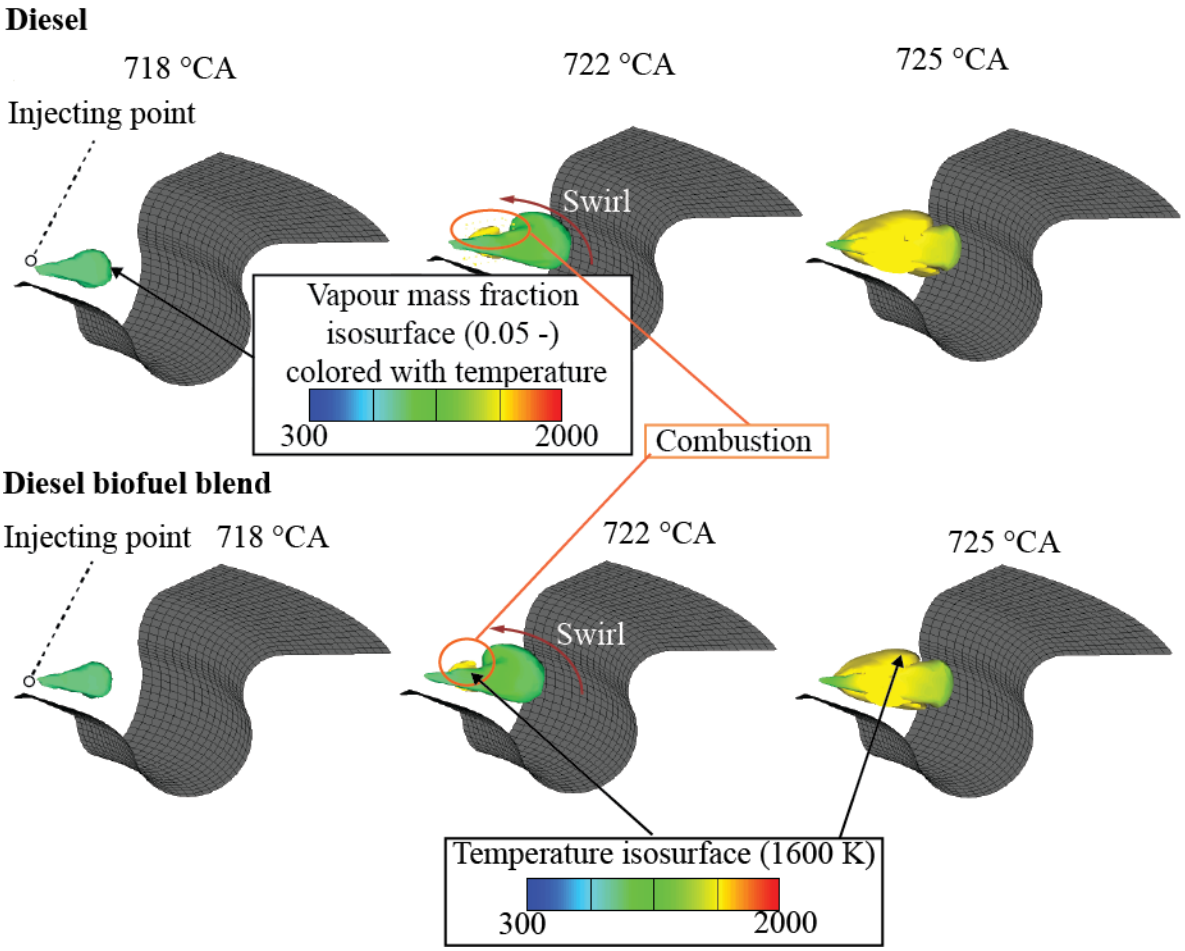

Figure 13 Comparison of calculated vapour fuel development at start of the combustion process

In observed modelling cases, adding the 7% of biofuel to create a mixture with diesel result in a reduction of the overall NO emissions. Figure 7 shows the isosurfaces of the NO species, high-temperature regions and the vapour cloud at the developed spray state – 727 °CA. At this crank angle position, the liquid fuel is evaporated and the vapour cloud is spreading through the domain. The vapour cloud is swirled and mixed with the hot environment which finally leads to the combustion process. The black isosurface presents the vapour cloud whilst the yellow one presents the high-temperature region where a temperature higher than 1600 K is noticed. When such high temperatures are achieved, the triple bond of nitrogen molecule are broken and thermal NO is formed. Both modelling cases exhibit a similar behaviour where a larger high-temperature region is noticed for pure diesel fuel combustion, which ultimately leads to faster NO species formation.

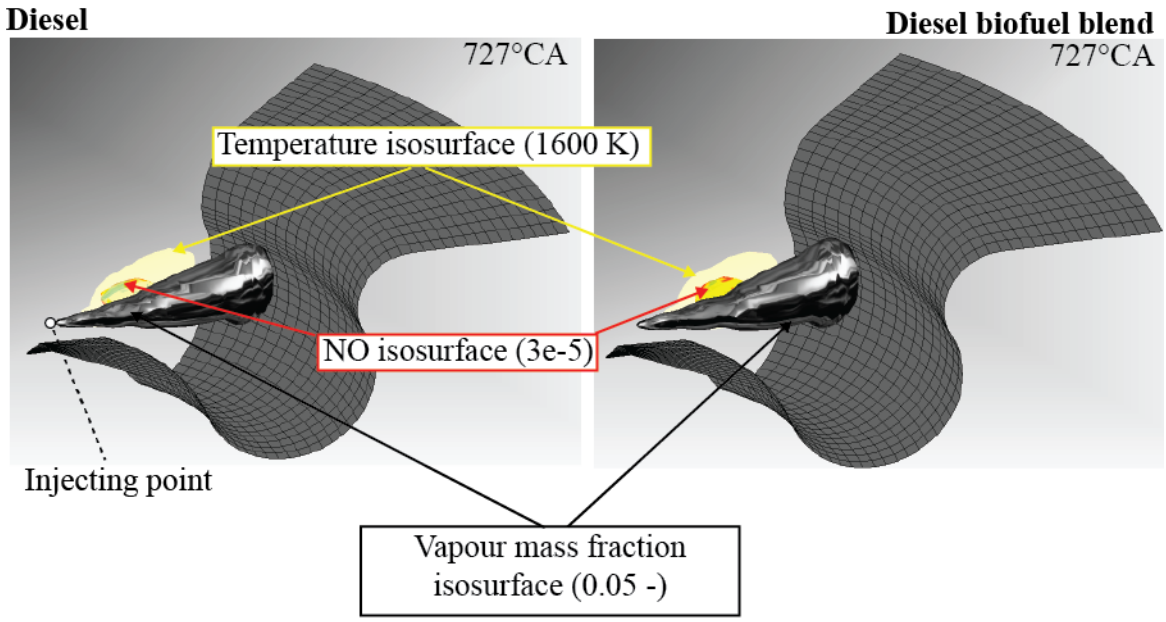

Figure 14 Comparison of calculated NO species at 727 °CA

6. CONCLUSION

Formation of pollutants during combustion in compression-ignition engines is a complex phenomenon depending on a range of parameters whose effect is hard to accurately estimate. Numerical modelling can serve as a valuable addition to the experimental investigations of different working conditions, geometries or fuel blends in the development of IC engines. This is especially true for the in-cylinder pollutant emission analysis, which is costly and problematic to observe in experimental setups, but of great interest when trying to optimise engine technologies to comply with the latest legislature.

Presented numerical model, implemented in the CFD code FIRE, covers all of the physics relevant to the pollutant emission. Spray, the effect of the flow field on it, as well as the disintegration of liquid fuel were modelled. Further, the process of fuel evaporation, ignition and combustion are included. Finally, the formation of emissions, both nitrogen-containing pollutants and the soot is covered by the model.

The model was validated by simulating the NO emissions over the range of operating conditions and comparing the data with experimental results. Furthermore, when biodiesel blend was used as a fuel, an average reduction in NO emissions of approximately 8% was found. This shows that a potential for the NO pollutant reduction in real IC engines exists, even with using biodiesel as fuel. Furthermore, these results indicate that the assumptions about the origin of the apparent increase of NO emissions in the experimental investigations might be correct, and that the differences in the operational parameters when comparing biodiesel blends and diesel could have caused the generally higher levels of NO for biodiesel. It can be concluded that under the identical conditions simulated in this work, biofuel powered IC engines produce less NO than the regular diesel ones. Further research should be directed at using detailed models for nitrogen-containing pollutant chemistry to obtain more accurate results for NO concentrations that could be used for the estimation of possible pollutant reduction when utilising biofuel blends.

ACKNOWLEDGEMENTS

The authors wish to thank the company AVL List GmbH, Graz, Austria for the financing and opportunity to work on the research project. Authors would also wish to thank the CFD Development group at AVL-AST, Graz, Austria, for their support.

REFERENCES

Baleta, J., Mikulčić, H., Vujanović, M., Petranović, Z., Duić, N., 2016. Numerical simulation of urea based selective non-catalytic reduction deNOx process for industrial applications. Energy Convers. Manag. 125, 59–69. doi:10.1016/j.enconman.2016.01.062

Cusidó, J.A., Cremades, L. V., 2012. Atomized sludges via spray-drying at low temperatures: An alternative to conventional wastewater treatment plants. J. Environ. Manage. 105, 61–65. doi:10.1016/j.jenvman.2012.03.053

Dukowicz, J., 1979. Quasi-steady droplet phase change in the presence of convection. Informal Rep. Los Alamos Sci. Lab. doi:10.2172/6012968

Dukowicz, J.K., 1980. A particle-fluid numerical model for liquid sprays. J. Comput. Phys. 35, 229–253. doi:10.1016/0021-9991(80)90087-X

Edelbauer, W., 2014. Coupling of 3D Eulerian and Lagrangian spray approaches in industrial combustion engine simulations. J. Energy Power Eng. 8, 190–200. doi:10.17265/1934-8975/2014.01.022

Energy Agency, I., 2015. CO2 Emissions From Fuel Combustion Highlights 2015.

Faeth, G.., Hsiang, L.-P., Wu, P.-K., 1995. Structure and breakup properties of sprays. Int. J. Multiph. Flow 21, 99–127. doi:10.1016/0301-9322(95)00059-7

Fenimore, C.P., 1971. Formation of nitric oxide in premixed hydrocarbon flames. Symp. Combust. 13, 373–380. doi:10.1016/S0082-0784(71)80040-1

FIRE manual 2013, 2013. . Graz.

Giakoumis, E.G., Rakopoulos, C.D., Dimaratos, A.M., Rakopoulos, D.C., 2012. Exhaust emissions of diesel engines operating under transient conditions with biodiesel fuel blends. Prog. Energy Combust. Sci. 38, 691–715. doi:10.1016/j.pecs.2012.05.002

Guan, B., Zhan, R., Lin, H., Huang, Z., 2015. Review of the state-of-the-art of exhaust particulate filter technology in internal combustion engines. J. Environ. Manage. doi:10.1016/j.jenvman.2015.02.027

Hanjalić, K., Popovac, M., Hadžiabdić, M., 2004. A robust near-wall elliptic-relaxation eddy-viscosity turbulence model for CFD. Int. J. Heat Fluid Flow 25, 1047–1051. doi:10.1016/j.ijheatfluidflow.2004.07.005

Hill, S.C., Smoot, L.D., 2000. Modeling of nitrogen oxides formation and destruction in combustion systems. Prog. Energy Combust. Sci. 26, 417–458. doi:10.1016/S0360-1285(00)00011-3

Katrašnik, T., 2007. Hybridization of powertrain and downsizing of IC engine – A way to reduce fuel consumption and pollutant emissions – Part 1. Energy Convers. Manag. 48, 1411–1423. doi:10.1016/j.enconman.2006.12.004

Khair, K.M., Majewski, W.A., 2006. Diesel Emissions and Their Control. SAE International.

Klemeš, J.J., Varbanov, P.S., Huisingh, D., 2012. Recent cleaner production advances in process monitoring and optimisation. J. Clean. Prod. 34, 1–8. doi:10.1016/j.jclepro.2012.04.026

Kozarac, D., Vuilleumier, D., Saxena, S., Dibble, R.W., 2014. Analysis of benefits of using

internal exhaust gas recirculation in biogas-fueled HCCI engines. Energy Convers. Manag. 87, 1186–1194. doi:10.1016/j.enconman.2014.04.085

Lapuerta, M., Armas, O., Rodríguez-Fernández, J., 2008. Effect of biodiesel fuels on diesel engine emissions. Prog. Energy Combust. Sci. 34, 198–223. doi:10.1016/j.pecs.2007.07.001

Martin Sommerfeld, Berend van Wachem, R.O. (Ed.), 2008. Best Practice Guidelines for Computational Fluid Dynamics of Dispersed Multiphase Flows.

Mikulčić, H., von Berg, E., Vujanović, M., Wang, X., Tan, H., Duić, N., 2016. Numerical evaluation of different pulverized coal and solid recovered fuel co-firing modes inside a large-scale cement calciner. Appl. Energy 184, 1292–1305. doi:10.1016/j.apenergy.2016.05.012

Miller, J.A., Bowman, C.T., 1989. Mechanism and modeling of nitrogen chemistry in combustion. Prog. Energy Combust. Sci. 15, 287–338. doi:10.1016/0360-1285(89)90017-8

Mobasheri, R., Peng, Z., Mirsalim, S.M., 2012. Analysis the effect of advanced injection strategies on engine performance and pollutant emissions in a heavy duty DI-diesel engine by CFD modeling. Int. J. Heat Fluid Flow 33, 59–69. doi:10.1016/j.ijheatfluidflow.2011.10.004

Naber, J., Reitz, R.D., 1988. Modeling Engine Spray/Wall Impingement. doi:10.4271/880107

Niemisto, J., Saavalainen, P., Pongracz, E., Keiski, R.L., 2013. Biobutanol as a Potential Sustainable Biofuel - Assessment of Lignocellulosic and Waste-based Feedstocks. J. Sustain. Dev. Energy, Water Environ. Syst. 1, 58–77.

Nordin, N., 2001. Complex Chemistry Modeling of Diesel Spray Combustion, CTH. Chalmers University of Technology.

O'Rourke, P.J., 1989. Statistical properties and numerical implementation of a model for droplet dispersion in a turbulent gas. J. Comput. Phys. 83, 345–360. doi:10.1016/0021-9991(89)90123-X

Petranović, Z., Edelbauer, W., Vujanović, M., Duić, N., 2017. Modelling of spray and combustion processes by using the Eulerian multiphase approach and detailed chemical kinetics. Fuel 191, 25–35. doi:10.1016/j.fuel.2016.11.051

Petranović, Z., Vujanović, M., Duić, N., 2015. Towards a more sustainable transport sector by numerically simulating fuel spray and pollutant formation in diesel engines. J. Clean. Prod. 88, 272–279. doi:10.1016/j.jclepro.2014.09.004

Reitz, R.D., 1987. Modeling atomization processes in high-pressure vaporizing sprays. At. Spray Technol. 3, 309–337.

Scheffknecht, G., Al-Makhadmeh, L., Schnell, U., Maier, J., 2011. Oxy-fuel coal combustion-A review of the current state-of-the-art. Int. J. Greenh. Gas Control 5, 16–35. doi:10.1016/j.ijggc.2011.05.020

Schiller, L., Naumann, Z., 1933. A drag coefficient correlation. Z.Ver.Deutsch.Ing 77, 318–320. doi:10.1016/j.ijheatmasstransfer.2009.02.006

Sun, J., Caton, J.A., Jacobs, T.J., 2010. Oxides of nitrogen emissions from biodiesel-fuelled diesel engines. Prog. Energy Combust. Sci. 36, 677–695. doi:10.1016/j.pecs.2010.02.004

Tashtoush, G.M., Al-Widyan, M.I., Albatayneh, A.M., 2007. Factorial analysis of diesel engine performance using different types of biofuels. J. Environ. Manage. 84, 401–411. doi:10.1016/j.jenvman.2006.06.017

Vallet, A., Burluka, A.A., Borghi, R., 2001. Development of a Eulerian Model for the "Atomization" of a Liquid Jet. At. Sprays 11, 24. doi:10.1615/AtomizSpr.v11.i6.20

von Berg, E., Edelbauer, W., Alajbegovic, A., Tatschl, R., Volmajer, M., Kegl, B., Ganippa, L.C., 2005. Coupled Simulations of Nozzle Flow, Primary Fuel Jet Breakup, and Spray Formation. J. Eng. Gas Turbines Power 127, 897. doi:10.1115/1.1914803

Vujanović, M., 2010. Numerical modelling of multiphase flow in combustion of liquid fuel. Fakultet strojarstva i brodogradnje, Sveučilište u Zagrebu.

Vujanović, M., Duić, N., Tatschl, R., 2009. Validation of reduced mechanisms for nitrogen chemistry in numerical simulation of a turbulent non-premixed flame. React. Kinet. Catal. Lett. 96, 125–138. doi:10.1007/s11144-009-5463-2

Vujanović, M., Petranović, Z., Edelbauer, W., Duić, N., 2016. Modelling spray and combustion processes in diesel engine by using the coupled Eulerian–Eulerian and Eulerian–Lagrangian method. Energy Convers. Manag. doi:10.1016/j.enconman.2016.03.072

Zeldovich, Y.A., Frank-Kamenetskii, D., Sadovnikov, P., 1947. Oxidation of nitrogen in combustion. Publishing House of the Acad of Sciences of USSR.